



## Review article

# A comprehensive overview on the synthesis, structures and applications of mono-nuclear transition metal complexes with asymmetrically substituted ‘salen-type’ Schiff bases

Puspender Middya<sup>a</sup>, Aritra Saha<sup>b</sup>, Shouvik Chattopadhyay<sup>a,\*</sup>

<sup>a</sup> Department of Chemistry, Jadavpur University, Kolkata 700032, India

<sup>b</sup> ISERC, Visva-Bharati, West Bengal, India



## ARTICLE INFO

**Keywords:**

Asymmetric Schiff base, transition metal  
Synthetic strategy  
Structure  
Application

## ABSTRACT

Salen-type ligands, prepared by the 1:2 condensation of a diamine and a salicylaldehyde derivative, represent a well known class of symmetrical tetra-dentate ligands, which have been used in the synthesis of a variety of complexes with several transition metals since long. Syntheses of ‘salen type’ asymmetric Schiff base ligands containing two different salicylaldehyde moieties, on the other hand, are tricky. This review focuses light on the synthesis of different ‘salen type’ asymmetric Schiff base ligands, and their mono-nuclear transition metal complexes. The X-ray structures and application of these complexes are also discussed.

## 1. Introduction

The widely used symmetrical tetradeinate  $\text{N}_2\text{O}_2$  donor bis(salicylidene) Schiff base ligands (commonly known as  $\text{H}_2\text{salen}$ ) have been synthesized by the 1:2 condensation of any primary diamine with any salicylaldehyde derivative [1–12]. Their enduring popularity may be related to the fact that they could be prepared very easily. The stability of the Schiff bases may also be another important reason. On the other hand, the most common geometry of a transition metal is octahedral and these tetra-dentate Schiff bases may occupy only four coordination sites of the metal ions leaving two sites free for coordination with other ligands [13]. In most of the complexes, the  $\text{N}_2\text{O}_2$  donor Schiff bases occupy the equatorial positions and axial positions are occupied by two mono-dentate ligands forming *trans* isomers as the main product [14,15]. On the other hand, in some limited complexes, the  $\text{N}_2\text{O}_2$  donor Schiff bases may occupy three equatorial positions and one axial position, whereas two *cis* positions are occupied by two mono-dentate ligands or a chelating bi-dentate ligand forming the *cis* isomer [16,17]. The bridging ability of the phenoxy oxygen atoms may also be utilised for the synthesis of poly-nuclear complexes [7,18–29]. We have already written several reviews on the synthesis, structures and properties transition metal complexes with these salen type ligands [30–32].

In these salen type symmetrical tetra-dentate ligands, same electronic and steric contributions are imposed by salicylaldehyde moieties

on both sides of the diamine. On the other hand, two different salicylaldehyde moieties are condensed with the diamine in an asymmetric (salen type) Schiff base [33–49]. This may allow tuning of the electronic and steric effects on each side of the Schiff base and may lead to the designed synthesis of new functional materials having potential to be used in energy-storage, sensory, and optoelectronic devices. These asymmetric (salen type) Schiff bases are also used in non-linear optical devices [50], catalytic systems [51], and in creating models of biological systems [52,53]. The complexes of these asymmetric Schiff bases are also more promising to be used as catalysis for oxidase reactions [7] and as single molecule magnets [54]. However, in comparison to the large number of complexes of symmetrical salen type Schiff bases, complexes of asymmetrical (salen type) Schiff bases are limited, presumably because of the inherent difficulties in their synthesis. When one of the carbonyl compounds is acetylacetone or its derivatives, asymmetric di-condensation of the diamines could be performed under high dilution technique to form asymmetric Schiff bases [55]. This process has also been used by several groups using two aromatic carbonyl compounds (e.g. salicylaldehyde and its derivatives). In this process, asymmetric (salen type) Schiff bases are synthesised via the formation of the half unit of the salen ligand (sometimes referred to as ‘half-salen’), which is nothing but the mono-condensation product of the reaction between a diamine and a carbonyl compound. There are few methods in the literature for the synthesis of the half unit species, but a template method in the presence

\* Corresponding author.

E-mail address: [shouvik.chattopadhyay@jadavpuruniversity.in](mailto:shouvik.chattopadhyay@jadavpuruniversity.in) (S. Chattopadhyay).

**Table 1**

Names and abbreviations of the Schiff base ligands included in this review.

Abbreviations	Names of ligands	Reference
H <sub>2</sub> L <sup>1</sup>	N-(salicylidene)-N'-(3-methoxysalicylidene)ethane-1,2-diamine	33
H <sub>2</sub> L <sup>2</sup>	N-(2'-hydroxy-5'-hydroxy-1-phenyl-1-phenylmethylidene)-N'-(salicylidene)ethane-1,2-diamine	39
H <sub>2</sub> L <sup>3</sup>	N-((2-hydroxynaphthalen-1-yl)methylidene)-N'-(2'-hydroxy-4'-hydroxy-1-phenyl-1-phenylmethylidene)ethane-1,2-diamine	39
H <sub>2</sub> L <sup>4</sup>	N-(2'-hydroxy-4'-hydroxy-1-phenyl-1-phenylmethylidene)-N'-(4'-hydroxy-salicylidene)ethane-1,2-diamine	39
H <sub>2</sub> L <sup>5</sup>	N-{1,1-bis(2'-hydroxyphenyl)methylidene}-N'-(3,5-di- <i>tert</i> -butylsalicylidene)ethane-1,2-diamine	46
H <sub>2</sub> L <sup>6</sup>	N-{1-phenyl-(2-hydroxy-4-(2-(piperidin-1-yl)ethoxy)-1-phenyl)methylidene}-N'-(2-hydroxynaphthalen-1-yl)methylidene)ethane-1,2-diamine	39
H <sub>2</sub> L <sup>7</sup>	N-3-ethoxysalicylidene-N'-3-methoxysalicylidene-1,3-propanediamine	34
H <sub>2</sub> L <sup>8</sup>	N-(2-hydroxynaphthal-1-methylidene)-N'-(3-methoxysalicylidene)propane-1,3-diamine	35
H <sub>2</sub> L <sup>9</sup>	N-(1-(2-hydroxyphenyl)ethylidene)-N'-(salicylidene)propane-1,3-diamine	41
H <sub>2</sub> L <sup>10</sup>	N-(1-(2-hydroxyphenyl)ethylidene)-N'-(5-bromosalicylidene)propane-1,3-diamine	35
H <sub>2</sub> L <sup>11</sup>	N-(1-(2-hydroxyphenyl)ethylidene)-N'-(3-methoxysalicylidene)propane-1,3-diamine	35
H <sub>2</sub> L <sup>12</sup>	N-(1-(2-hydroxyphenyl)ethylidene)-N'-(2-hydroxynaphthal-1-methylidene)propane-1,3-diamine	35
H <sub>2</sub> L <sup>13</sup>	N-(1-(2-hydroxyphenyl)ethylidene)-N'-(3- <i>tert</i> -butyl-5-methyl-salicylidene)-1,2-diamino-2-methylpropane	47
H <sub>2</sub> L <sup>14</sup>	N-(1-(2-hydroxyphenyl)ethylidene)-N'-(2-hydroxynaphthal-1-methylidene)-1,2-diamino-2-methylpropane	42
H <sub>2</sub> L <sup>15</sup>	N-(1-(2-hydroxyphenyl)ethylidene)-N'-(3,5-di- <i>tert</i> -butylsalicylidene)-1,2-diamino-2-methylpropane	43
H <sub>2</sub> L <sup>16</sup>	N-(1-(3,5-di- <i>tert</i> -butyl-1-hydroxyphenyl)ethylidene)-N'-(3- <i>tert</i> -butyl-5-phenylsalicylidene)-1,2-diamino-2-methylpropane	44, 48
H <sub>2</sub> L <sup>17</sup>	N-(1-(2-hydroxyphenyl)ethylidene)-N'-(salicylidene)cyclohexane-1,2-diamine	36
H <sub>2</sub> L <sup>18</sup>	N-(1-(2-hydroxyphenyl)ethylidene)-N'-(3,5-di- <i>tert</i> -butylsalicylidene)cyclohexane-1,2-diamine	46
H <sub>2</sub> L <sup>19</sup>	N-(salicylidene)-N'-(2-hydroxynaphthalen-1-yl)methylene)cyclohexane-1,2-diamine	36, 49
H <sub>2</sub> L <sup>20</sup>	N-(salicylidene)-N'-(3-methoxysalicylidene)-1,2-diphenyl-1,2-ethylenediamine	38

of the desired metal ion is probably the easiest and most widely used.

In this review, we shall focus on the synthesis, structure and properties of mono-nuclear complexes of transition metals with asymmetric (salen type) Schiff bases [33–49]. The syntheses of the ligands are also discussed. We have included the structures of the complexes from the Cambridge Crystallographic Data Centre (CCDC).

## 2. Synthetic strategy

In this review, we have discussed the syntheses and crystal structures of mono-nuclear complexes of different transition metals with (salen type) asymmetric Schiff base ligands (Table 1), reported by different researchers. Schemes 1–3 gather molecular formula/structural molecular diagrams of the ligands.

### 2.1. Synthesis of ligands

Two different methods have been followed for the synthesis of the ligands, viz. (i) To synthesize of mono-condensed Schiff base at low temperature and at high dilution condition in the first step and then formation of the asymmetric Schiff base in the second step, and (ii) To

form (and then precipitate out) Ni(DMG)<sub>2</sub> to prepare the asymmetric Schiff base [33,34,38,41]. The first process is always giving mixtures of one unsymmetrical and two symmetrical salen type Schiff base ligands. In the second process, there is always a possibility of having symmetrical Schiff base, especially if sufficient time is allowed to reach the equilibrium. This has been confirmed by the mass spectral analysis in most of the cases. This is not surprising, since the imine bonds are reversible. However, separation of the symmetrical and unsymmetrical Schiff bases is therefore necessary prior to their use as ligands in synthesis of the complexes. This is the most serious drawbacks of these two methods. Therefore, the best way of synthesizing transition metal complexes of unsymmetrical Schiff bases is to prepare the ligand *in situ*, as was done for the synthesis of H<sub>2</sub>L<sup>1</sup>, H<sub>2</sub>L<sup>7</sup>, H<sub>2</sub>L<sup>9</sup> and H<sub>2</sub>L<sup>20</sup> (vide infra). They were not isolated from the solution and were prepared *in situ* during the preparation of corresponding copper(II) and nickel(II) complexes.

#### 2.1.1. Synthesis of mono-condensed Schiff base at low temperature and at high dilution condition in the first step and then formation of the asymmetric Schiff base in the second step

**2.1.1.1. Synthesis of H<sub>2</sub>L<sup>2</sup>, H<sub>2</sub>L<sup>3</sup> and H<sub>2</sub>L<sup>4</sup>.** A solution of 2,4-dihydroxybenzophenone in methanol was slowly added to a solution of 1,2-diaminoethane in methanol, and refluxing the reaction mixture for 16 h to prepare the mono-condensed Schiff base ligand. Salicylaldehyde, 2-hydroxynaphthaldehyde or 2,4-dihydroxybenzaldehyde dissolved in methanol was then slowly added to a suspension of the mono-condensed Schiff base ligand in methanol under reflux to give a transparent yellow solution of H<sub>2</sub>L<sup>2</sup>, H<sub>2</sub>L<sup>3</sup> and H<sub>2</sub>L<sup>4</sup> respectively [39]. The synthetic routes of ligands H<sub>2</sub>L<sup>2</sup>, H<sub>2</sub>L<sup>3</sup>, and H<sub>2</sub>L<sup>4</sup> have been shown in Scheme 4.

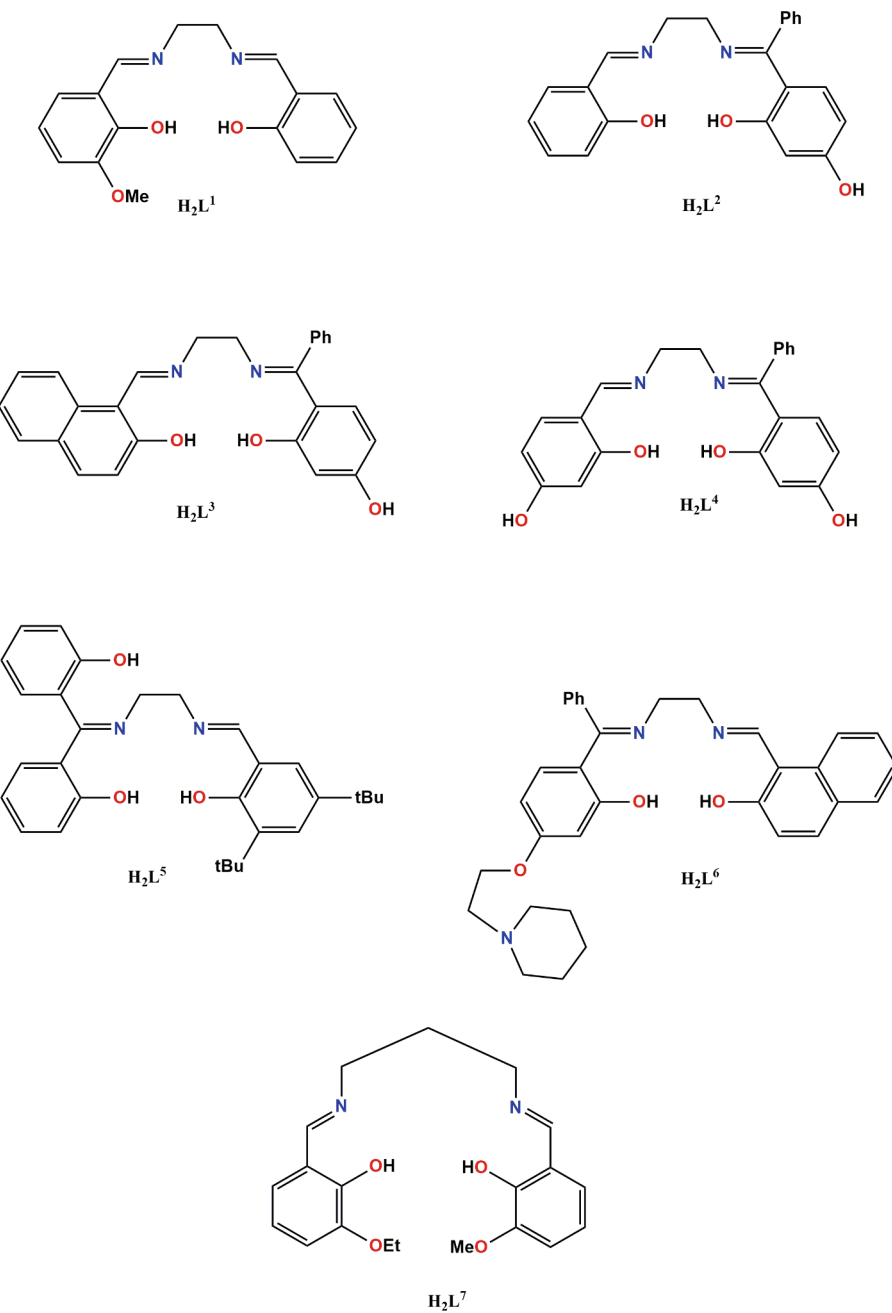
**2.1.1.2. Synthesis of H<sub>2</sub>L<sup>5</sup>.** A methanol solution of 1,2-diaminoethane with 2,2'-dihydroxybenzophenone was heated to synthesize the corresponding mono-condensed Schiff base as a yellow precipitate. A methanol solution of 3,5-di-*tert*-butyl-2-hydroxybenzaldehyde was then added to a stirred suspension of the yellow material in methanol with constant stirring, followed by the addition of diethyl ether to get the asymmetric Schiff base, H<sub>2</sub>L<sup>5</sup> [46] as a yellow solid. The synthetic route of H<sub>2</sub>L<sup>5</sup> has been shown in Scheme 5.

**2.1.1.3. Synthesis of H<sub>2</sub>L<sup>6</sup>.** Mono-condensed Schiff base ligand was prepared by adding a methanol solution of 2-hydroxynaphthaldehyde to a methanol solution of 1,2-diaminoethane under refluxed. A methanol solution of (2-hydroxy-4-(2-(piperidin-1-yl)ethoxy)phenyl)(phenyl)methanone was then added to a suspension of the mono-condensed Schiff base ligand in methanol to give the asymmetric Schiff base, H<sub>2</sub>L<sup>6</sup> [39]. The synthetic route to H<sub>2</sub>L<sup>6</sup> has been shown in Scheme 6.

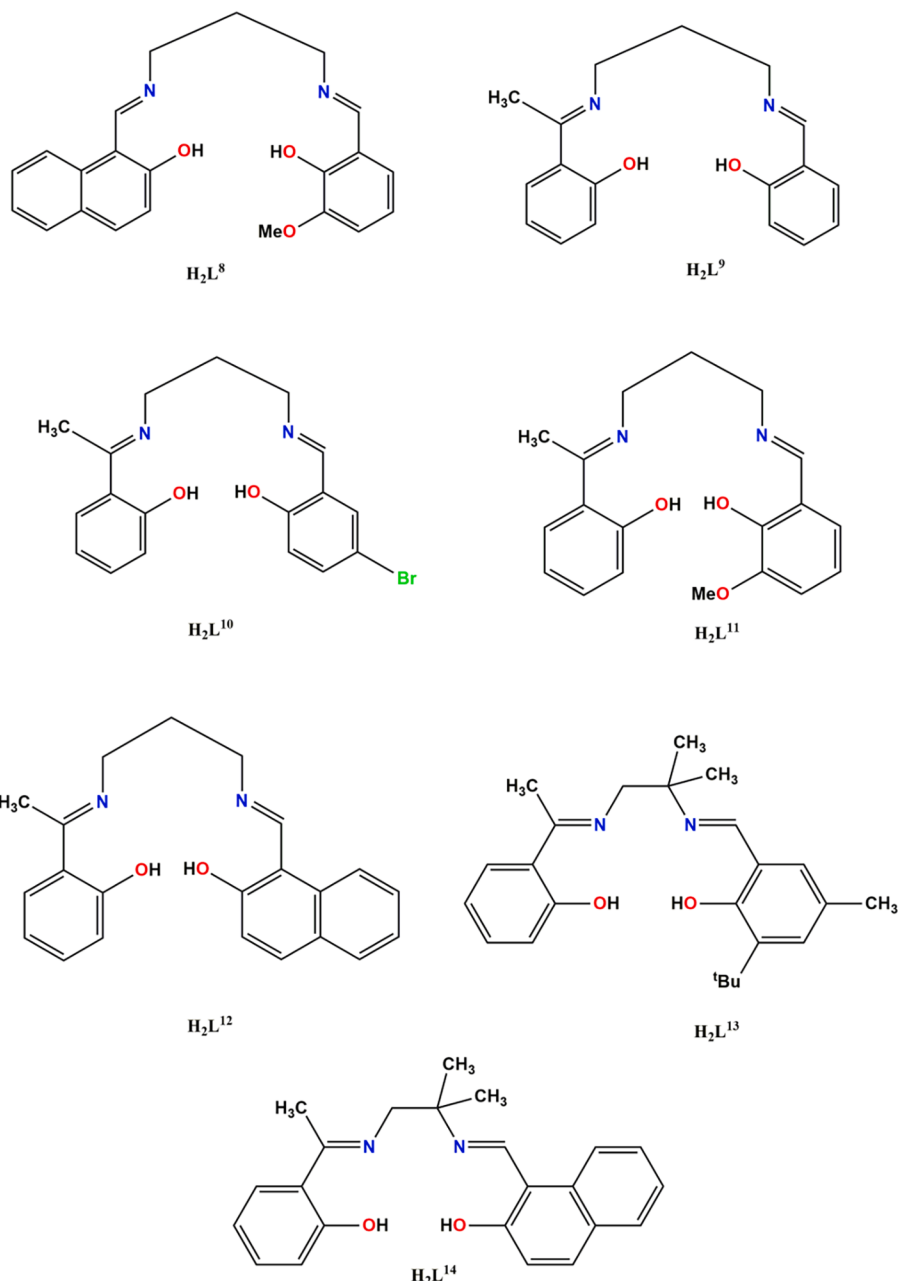
**2.1.1.4. Synthesis of H<sub>2</sub>L<sup>13</sup>.** A methanol solution of 2-hydroxyacetophenone and 1,2-diamino-2-methylpropane was refluxed to synthesize the mono-condensed Schiff base, which on refluxing with a methanol solution of 3-*tert*-butyl-5-methylsalicylaldehyde produced the Schiff base H<sub>2</sub>L<sup>13</sup> [47] which was crystallized from hot petroleum ether. The synthetic route has been shown in Scheme 7.

**2.1.1.5. Synthesis of H<sub>2</sub>L<sup>14</sup> and H<sub>2</sub>L<sup>15</sup>.** A DCM solution of 2-hydroxyacetophenone and 2-amino-2-methylpropylamine were refluxed for half an hour with constant stirring, then the evaporation of the solvent yielded a yellow color mono-condensed Schiff base. The diethyl ether solution of 2-hydroxynaphthaldehyde and 2-hydroxy-3,5-di-*tert*-butylbenzaldehyde were added to mono-condensed Schiff base to prepared asymmetric Schiff base ligand H<sub>2</sub>L<sup>14</sup> and H<sub>2</sub>L<sup>15</sup> [42,43]. The synthetic route has been shown in Scheme 8.

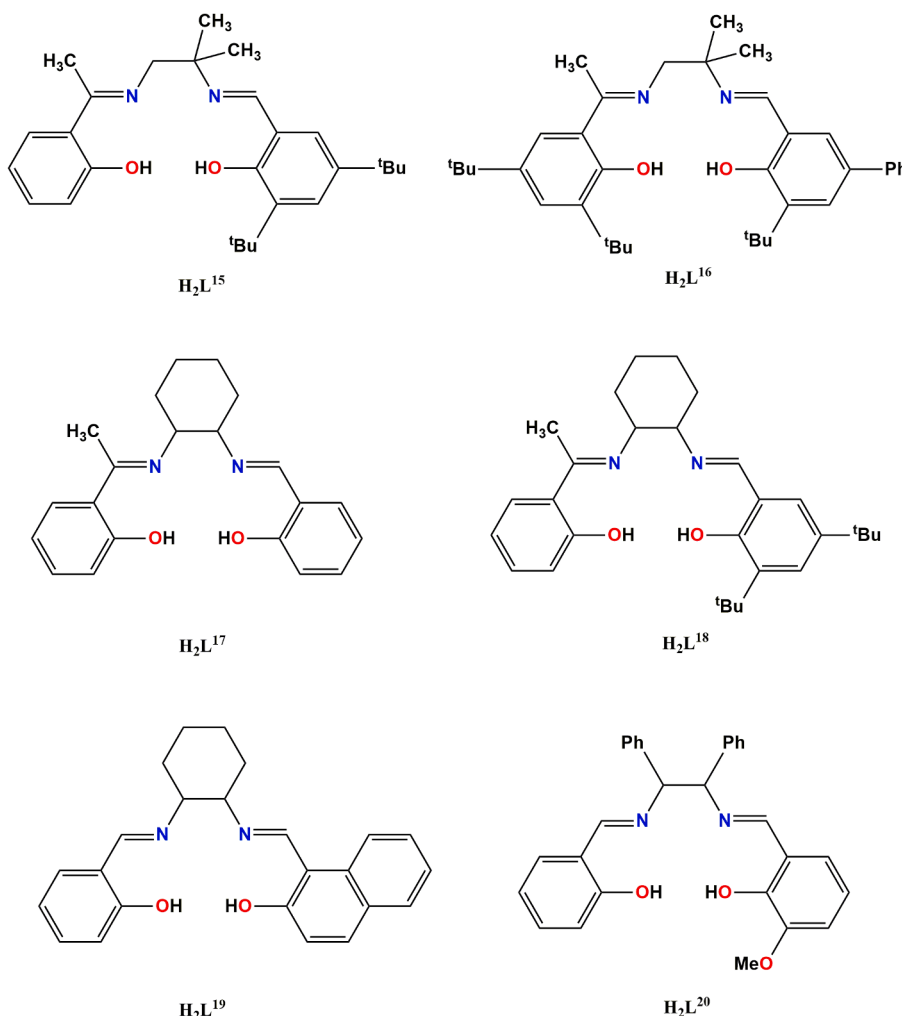
**2.1.1.6. Synthesis of H<sub>2</sub>L<sup>16</sup>.** The mono condensed Schiff base was first



**Scheme 1.** Schematic representation of the ligands, H<sub>2</sub>L<sup>1</sup>-H<sub>2</sub>L<sup>7</sup>.



**Scheme 2.** Schematic representation of the ligands,  $\text{H}_2\text{L}^8\text{-H}_2\text{L}^{14}$ .



**Scheme 3.** Schematic representation of the ligands,  $H_2L^{15}$ - $H_2L^{20}$ .

prepared by adding a methanol solution of 2-acetyl-3,5-di-*tert*-butylphenol into a methanol solution of 2-amino-2-methylpropylamine. Then this mono-condensed Schiff base was added to a methanol solution of 5-phenyl-3-*tert*-butylsalicylaldehyde under reflux with stirring to obtain the asymmetric Schiff base,  $H_2L^{16}$  [44]. The synthetic route has been shown in Scheme 9.

**2.1.1.7. Synthesis of  $H_2L^{17}$ .** An ethanol solution of 1,2-diaminohexane was added to an ethanol solution of 2-hydroxyacetophenone with stirring at room temperature. Salicylaldehyde in ethanol was then added with constant stirring to synthesize the yellow solution of  $H_2L^{17}$  [36]. The synthetic route of  $H_2L^{17}$  has been shown in scheme 10.

**2.1.1.8. Synthesis of  $H_2L^{18}$ .** The mono-condensed Schiff base ligand was prepared by adding a chloroform solution of 2-hydroxy-3,5-di-*tert*-butylbenzaldehyde and 1,2-diaminocyclohexane (1:1 M ratio) with stirring at 0 °C, then the reaction mixture warmed up to room temperature. The asymmetric Schiff base ligand ( $H_2L^{18}$ ) [45] was obtained by addition of an ethanol solution of 2-hydroxyacetophenone to the mono-condensed Schiff base ligand (equal molar ratio). The synthetic route of  $H_2L^{18}$  has been shown in Scheme 11.

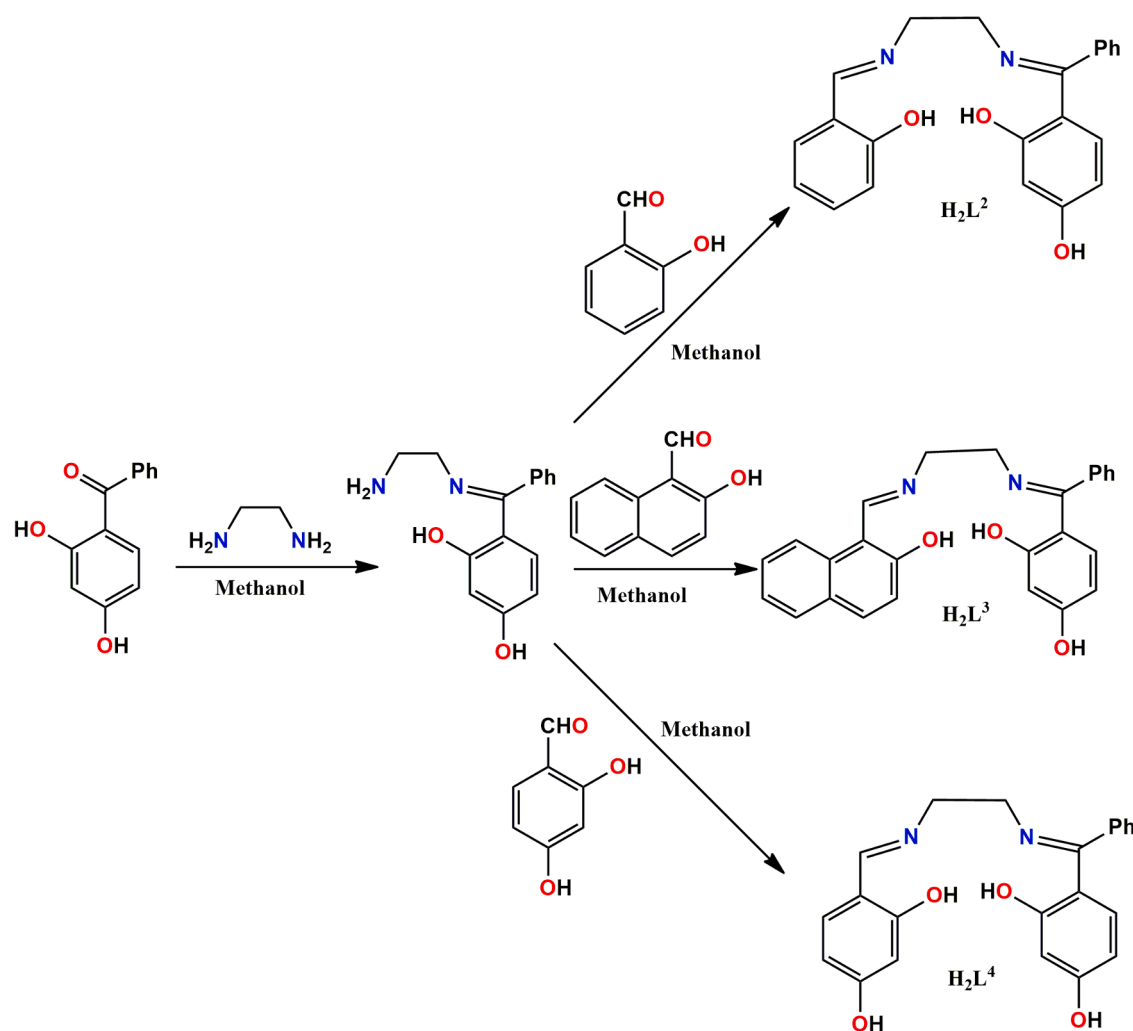
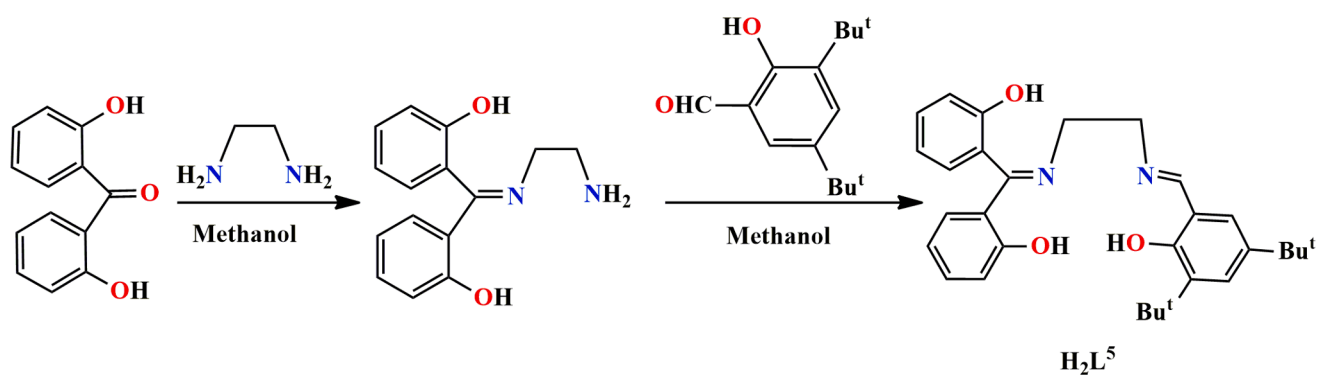
**2.1.1.9. Synthesis of  $H_2L^{19}$ .** An anhydrous ethanol solution of 2-hydroxynaphthaldehyde was added dropwise in to the ethanol solution of *trans*-1,2-cyclohexanediamine at 0 °C with constant stirring to get the mono-condensed Schiff base ( $HL^P$ ). The asymmetric Schiff base,  $H_2L^{19}$  [23],

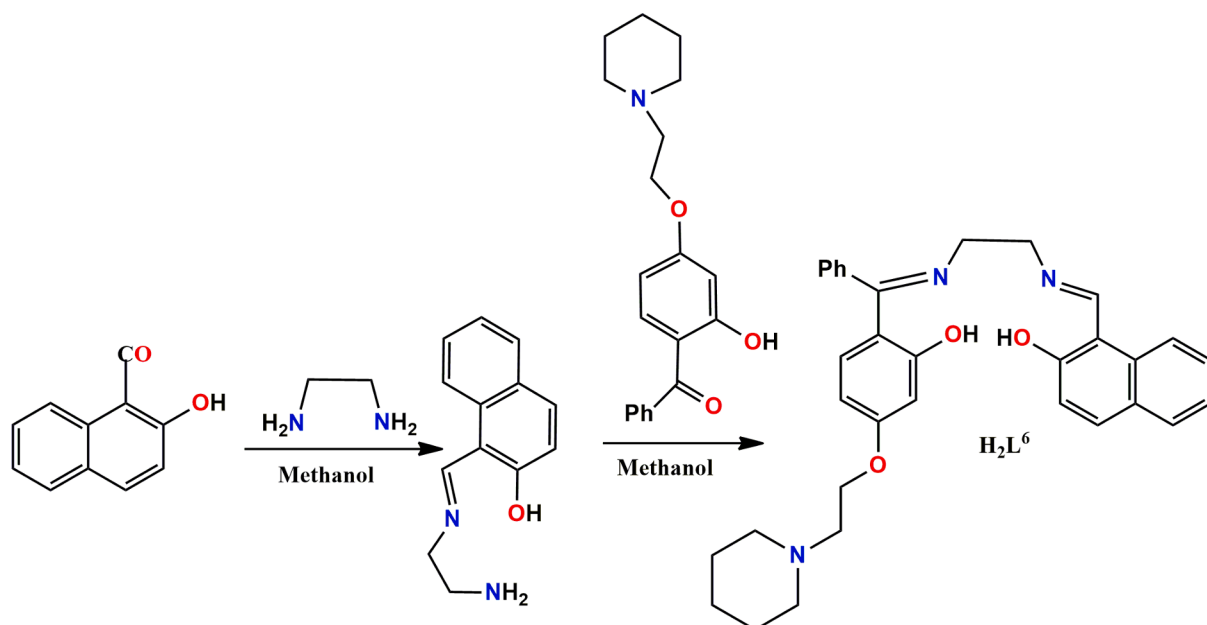
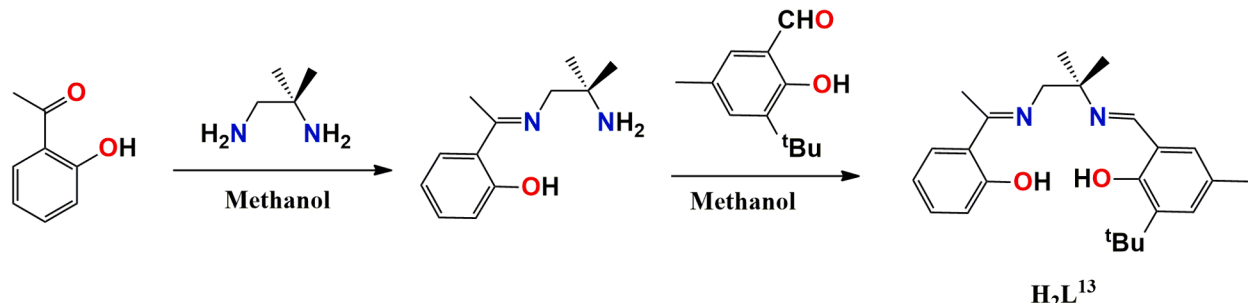
was obtained by the reaction of mono-condensed Schiff base and an ethanol solution of salicylaldehyde. The synthetic route of  $H_2L^{19}$  has been shown in Scheme 12.

#### 2.1.2. Formation of $Ni(DMG)_2$ as the driving force to prepare the asymmetric Schiff base

**2.1.2.1. Synthesis of  $H_2L^8$ .** A methanol solution of  $Ni(L^a)_2$  { $HL^a = 3$ -methoxysalicylaldehyde} and  $Ni(L^b)_2$  { $HL^b = 2$ -hydroxynaphthaldehyde} was refluxed with excess 1,3-propanediamine in methanol to prepare the di-nuclear complex  $[Ni_2(L)_2(L^b)_2]$  { $HL = 2$ -(2-(3-amino-propylimino)ethyl)-6-methoxyphenol}, which was collected by filtration. De-metallation of the complex using excess solid dimethylglyoxime (HDMG) in methanol under reflux on a water-bath, and filtering off the precipitate of  $Ni(DMG)_2$  produced the free asymmetric ligand,  $H_2L^8$  [35]. The synthetic route of the ligand  $H_2L^8$  has been shown in Scheme 13.

**2.1.2.2. Synthesis of  $H_2L^{10}$ ,  $H_2L^{11}$  and  $H_2L^{12}$ .** These ligands have been synthesized in a similar method using a methanol solution of  $[Ni(L^c)_2]$  { $HL^c = 2$ -hydroxyacetophenone} with  $[Ni(L^d)_2]$  { $HL^d = 5$ -bromosalicylaldehyde},  $[Ni(L^g)_2]$  { $HL^g = 3$ -methoxysalicylaldehyde} and  $[Ni(L^i)_2]$  { $HL^i = o$ -hydroxynaphthaldehyde} respectively. The synthetic routes to  $H_2L^{10}$ ,  $H_2L^{11}$  and  $H_2L^{12}$  [35] have been shown in Schemes 14-16 respectively.

**Scheme 4.** Synthetic routes to ligands  $\text{H}_2\text{L}^2$ ,  $\text{H}_2\text{L}^3$  and  $\text{H}_2\text{L}^4$ .**Scheme 5.** The synthetic route to  $\text{H}_2\text{L}^5$ .

Scheme 6. Synthetic route to  $\text{H}_2\text{L}^6$ .Scheme 7. The synthesis of  $\text{H}_2\text{L}^{13}$ .

## 2.2. Synthesis of the complexes

### 2.2.1. Synthesis of copper(II) complexes

**2.2.1.1. Synthesis of  $[\text{CuL}^1(\text{H}_2\text{O})]$  (1).** An aqueous solution of copper (II) nitrate trihydrate was added to a solution of salicylaldehyde (in 1:1 M ratio) in methanol in presence of pyridine with constant stirring, followed by the addition of 1,2-diaminoethane to get a dark-violet solid, which was collected by filtration. It was then added to a methanol solution of 3-methoxysalicylaldehyde and aqueous NaOH with stirring to get green crystals of complex 1 [33]. The synthetic route of the complex 1 has been shown in Scheme 17.

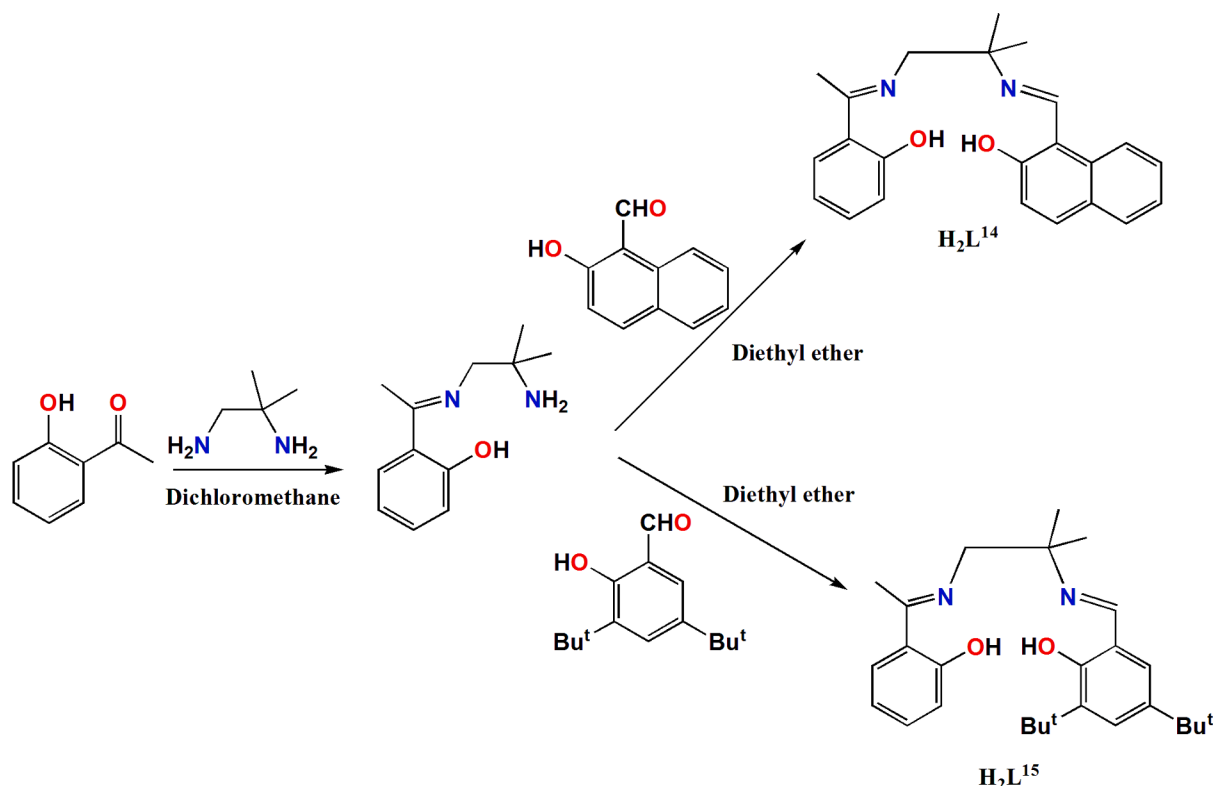
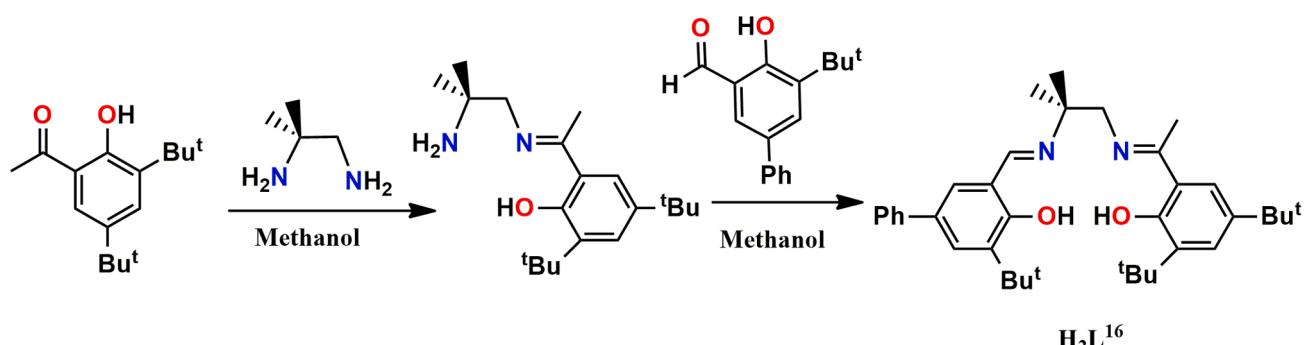
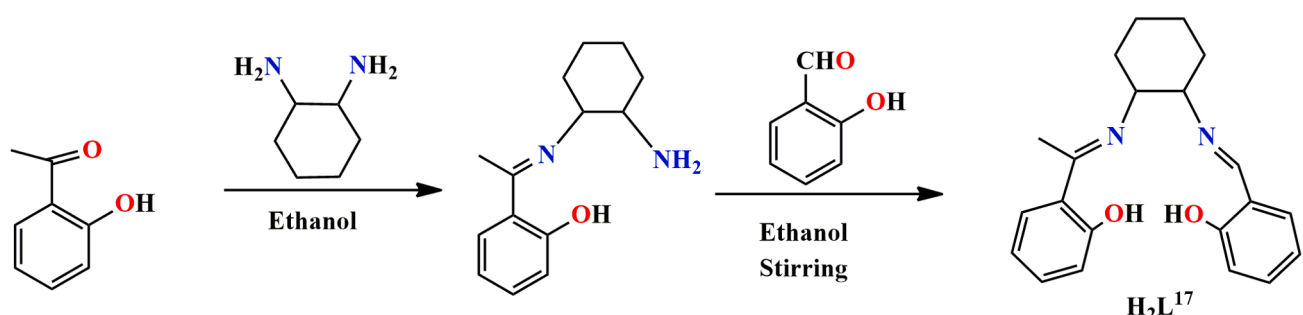
**2.2.1.2. Synthesis of  $[\text{CuL}^7 \cdot 3 \cdot 5\text{H}_2\text{O}]$  (2).** Solid bis(2-oxido-3-methoxybenzaldehyde)nickel(II) dihydrate was added to an ethanol solution of 1,3-diaminopropane under reflux, and the initial precipitate was filtered off. Yellow crystals, coming from the filtrate, were dissolved in methanol and solid bis(2-oxido-3-ethoxybenzaldehyde)copper(II) dihydrate was added under reflux to get green crystals of  $[\text{CuL}^7 \cdot 3 \cdot 5\text{H}_2\text{O}]$  (2) [34]. The synthetic route of the complex 2 has been shown in Scheme 18.

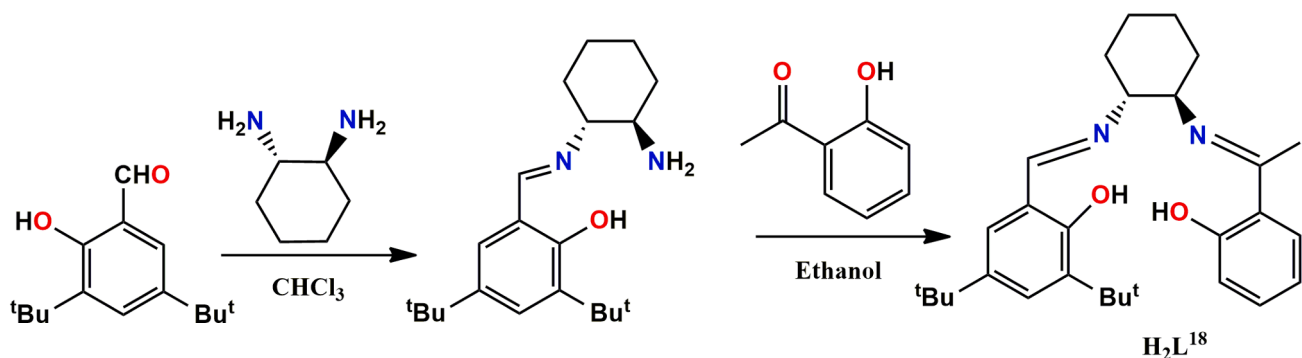
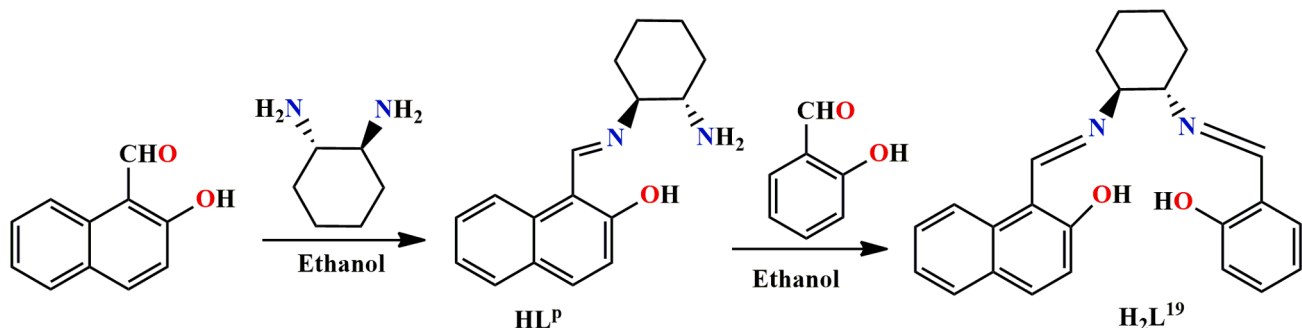
**2.2.1.3. Synthesis of  $[\text{CuL}^8(\text{H}_2\text{O})]$  (3),  $[\text{CuL}^{10}] \cdot 0.5\text{H}_2\text{O}$  (4),  $[\text{CuL}^{11}] \cdot \text{DCM}$  (5) and  $[\text{CuL}^{12}]$  (6).**  $[\text{CuL}^8(\text{H}_2\text{O})]$  (3) was synthesised by the reaction of methanol solution of copper(II) perchlorate hexahydrate in asymmetric ligand in methanol solution. Complexes 4, 5 and 6 were prepared in similar methods using the asymmetric Schiff base ligands,  $\text{H}_2\text{L}^{10}$ ,  $\text{H}_2\text{L}^{11}$  and  $\text{H}_2\text{L}^{12}$  respectively [35]. The synthetic routes of the complexes 3–6 have been outlined in Scheme 19.

**2.2.1.4. Synthesis of  $[\text{CuL}^{17}]$  (7).** An ethanol solution of copper(II) acetate monohydrate was then added to an ethanol solution of the Schiff base ligand  $\text{H}_2\text{L}^{17}$ ; and the mixture was kept undisturbed to yield green single crystals, suitable for X-ray diffraction [36]. The synthesis of the complex 7 is shown in Scheme 20.

**2.2.1.5. Synthesis of  $[\text{CuL}^{19}] \cdot 0.5\text{EtOH} \cdot 1.25\text{H}_2\text{O}$  (8).** An ethanol solution of copper(II) acetate was added to an ethanol solution of  $\text{H}_2\text{L}^{19}$  with constant stirring produced  $[\text{CuL}^{19}] \cdot 0.5\text{EtOH} \cdot 1.25\text{H}_2\text{O}$  (8) [37]. The synthesis of the complex 8 is shown in Scheme 21.

**2.2.1.6. Synthesis of  $[\text{CuL}^{20}]$  (9).** An aqueous solution of copper(II) perchlorate hexahydrate was added to a solution of 3-methoxysalicylaldehyde in methanol in presence of pyridine with constant stirring,

Scheme 8. The synthetic route to  $\text{H}_2\text{L}^{14}$  and  $\text{H}_2\text{L}^{15}$ .Scheme 9. Synthetic route to  $\text{H}_2\text{L}^{16}$ .Scheme 10. Synthesis route to  $\text{H}_2\text{L}^{17}$ .

Scheme 11. Synthetic route to  $\text{H}_2\text{L}^{18}$ .Scheme 12. Synthetic route to  $\text{H}_2\text{L}^{19}$ .

followed by the addition of 1,2-diphenyl-1,2-ethylenediamine to get a green solid, which was collected by filtration. It was then added to a methanol solution of the salicylaldehyde with stirring to get red crystal of complex **9** [38]. The synthetic route of the complex **9** has been shown in Scheme 22.

### 2.2.2. Synthesis of nickel(II) complexes

**2.2.2.1.  $[\text{NiL}^2]\cdot0.5\text{H}_2\text{O}$  (10),  $[\text{NiL}^3]\cdot2\text{H}_2\text{O}$  (11) and  $[\text{NiL}^4]\cdot\text{H}_2\text{O}$  (12).**  $\text{Ni(OAc)}_2\cdot4\text{H}_2\text{O}$  dissolved in methanol was added drop-wise to  $\text{H}_2\text{L}^1$ ,  $\text{H}_2\text{L}^2$  and  $\text{H}_2\text{L}^3$  respectively under reflux resulting in the formation of a dark orange complexes  $[\text{NiL}^2]\cdot0.5\text{H}_2\text{O}$  (10),  $[\text{NiL}^3]\cdot2\text{H}_2\text{O}$  (11) and  $[\text{NiL}^4]\cdot\text{H}_2\text{O}$  (12) [39]. The synthetic routes of complexes **10–12** have been shown in Scheme 23.

**2.2.2.2.  $[\text{NiL}^6]$  (13).** Nickel(II) acetate tetrahydrate dissolved in methanol was added to  $\text{H}_2\text{L}^6$  under reflux resulting in the formation of **13**, which was dark orange in colour [39]. The synthetic route of complex **13** has been shown in Scheme 24.

**2.2.2.3.  $[\text{NiL}^{11}]\cdot\text{DCM}$  (14).**  $[\text{NiL}^{11}]\cdot\text{DCM}$  (14) was obtained as a red crystalline product by the addition of a methanol solution of nickel(II) perchlorate hexahydrate to a methanol solution of  $\text{H}_2\text{L}^{11}$  with constant stirring. It was recrystallized from DCM solvent to get X-ray diffraction quality crystals of **14** [40]. The Synthetic route of the complex **14** has been shown in Scheme 25.

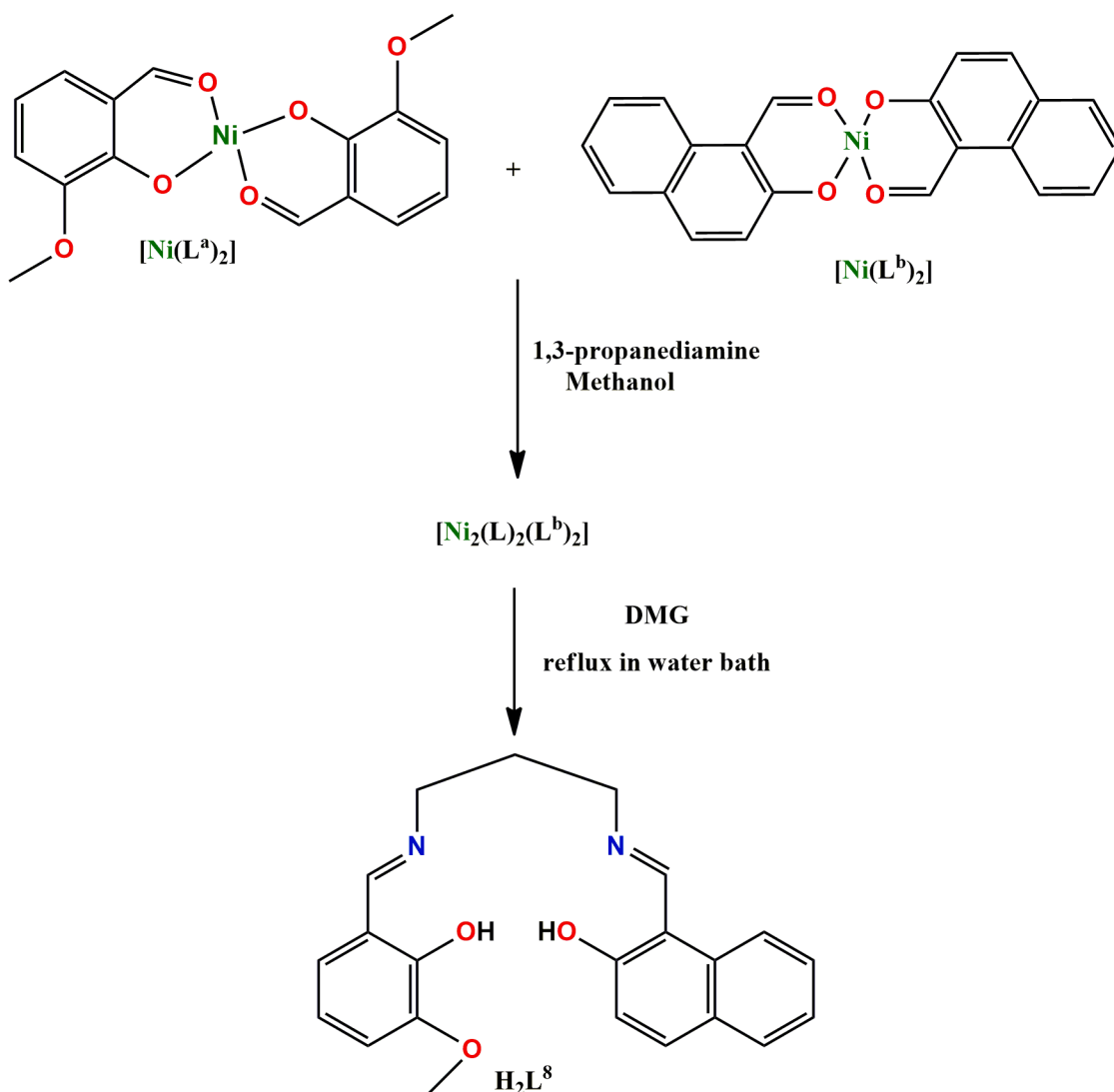
**2.2.2.4.  $[\text{NiL}^9]$  (15).** Solid bis(2-hydroxybenzaldehyde)nickel(II) dihydrate was added to a methanol solution of 1,3-diaminopropane under reflux, and the initial precipitate was filtered off. The crystals, coming from the filtrate, were dissolved in methanol and solid bis(2-hydroxyacetophenone)nickel(II) dihydrate was added under reflux to get deep red crystals of  $[\text{NiL}^9]$  (15) [41]. The synthetic route of the complex **15** has been shown in Scheme 27.

**2.2.2.5.  $[\text{NiL}^{14}]\cdot\text{CHCl}_3$  (16).**  $[\text{NiL}^{14}]\cdot\text{CHCl}_3$  (16) was synthesised by a chloroform solution of  $\text{H}_2\text{L}^{14}$  was added into the methanol solution of nickel(II) acetate tetrahydrate for 12 h with constant stirring [42]. The synthetic route of the complex **16** has been shown in Scheme 28.

**2.2.2.6.  $[\text{NiL}^{15}]\cdot\text{CHCl}_3$  (17).**  $[\text{NiL}^{15}]\cdot\text{CHCl}_3$  (17) was synthesised in a similar method using 2-hydroxy-3,5-di-*tert*-butylbenzaldehyde instead of 2-hydroxynaphthaldehyde [43]. The synthetic route of the complex **17** has been shown in Scheme 29.

**2.2.2.7.  $[\text{NiL}^{16}]\cdot0.39\text{DCM}$  (18).** A diethyl ether solution of  $\text{H}_2\text{L}^{16}$  was added into a methanol solution of nickel(II) acetate tetrahydrate followed by the addition of triethylamine with stirring to get complex **18** [44]. Olive green crystals of **18**, suitable for X-ray diffraction were obtained by the slow evaporation of the solvent. The synthetic route of the complex **18** has been shown in Scheme 30.

**2.2.2.8.  $[\text{NiL}^{18}]$  (19).**  $[\text{NiL}^{18}]$  (19) was prepared by adding an ethanol solution of nickel(II) acetate tetrahydrate to an ethanol solution of  $\text{H}_2\text{L}^{18}$

Scheme 13. Synthetic route to  $\text{H}_2\text{L}^8$ .

with constant stirring [45]. The synthetic route of complex **19** has been shown in Scheme 31.

#### 2.2.3. Synthesis of cobalt complexes

**2.2.3.1.  $[\text{Co}^{\text{II}}\text{L}^5(\text{R},\text{R-dpen})]\text{Tsa}\cdot 2\text{EtOH}$  (20)** [*dpen* = 1,2-diphenylethylenediamine; HTsa = *p*-toluenesulfonic acid]. A methanol solution of cobalt (II) acetate tetrahydrate was added to a stirred suspension of  $\text{H}_2\text{L}^5$  in methanol with constant stirring, followed by the addition of *p*-toluenesulfonic acid monohydrate (HTsa) in open atmosphere to get  $[\text{Co}^{\text{III}}\text{L}^5]\text{Tsa}$  as a dark green solid. A methanol solution of (R,R)-1,2-diphenylethylenediamine (R,R-dpen) was then added to a stirred solution of  $[\text{Co}^{\text{II}}\text{L}^5]\text{Tsa}$  with constant stirring to get  $[\text{Co}^{\text{V}}(\text{R},\text{R-deen})]\text{Tsa}$  as the final product. It is to be noted here the complex is optically active and pure  $\Delta$  isomer of the complex has been isolated by dissolving  $[\text{Co}^{\text{V}}(\text{deen})]\text{Tsa}$  in ethanol and then slowly adding pentane, and keeping the mixture at 5 °C [46]. The synthetic route of complex **20** has been shown in Scheme 32.

**2.2.3.2.  $[\text{Co}^{\text{II}}\text{L}^{13}]$  (21).** Reaction of cobalt(II) acetate tetrahydrate with the methanol solution of  $\text{H}_2\text{L}^{13}$  in presence of few drops of NaOH produced  $[\text{Co}^{\text{II}}\text{L}^{13}]$  (21) [47]. The synthetic route of the complex **21** has been shown in Scheme 33.

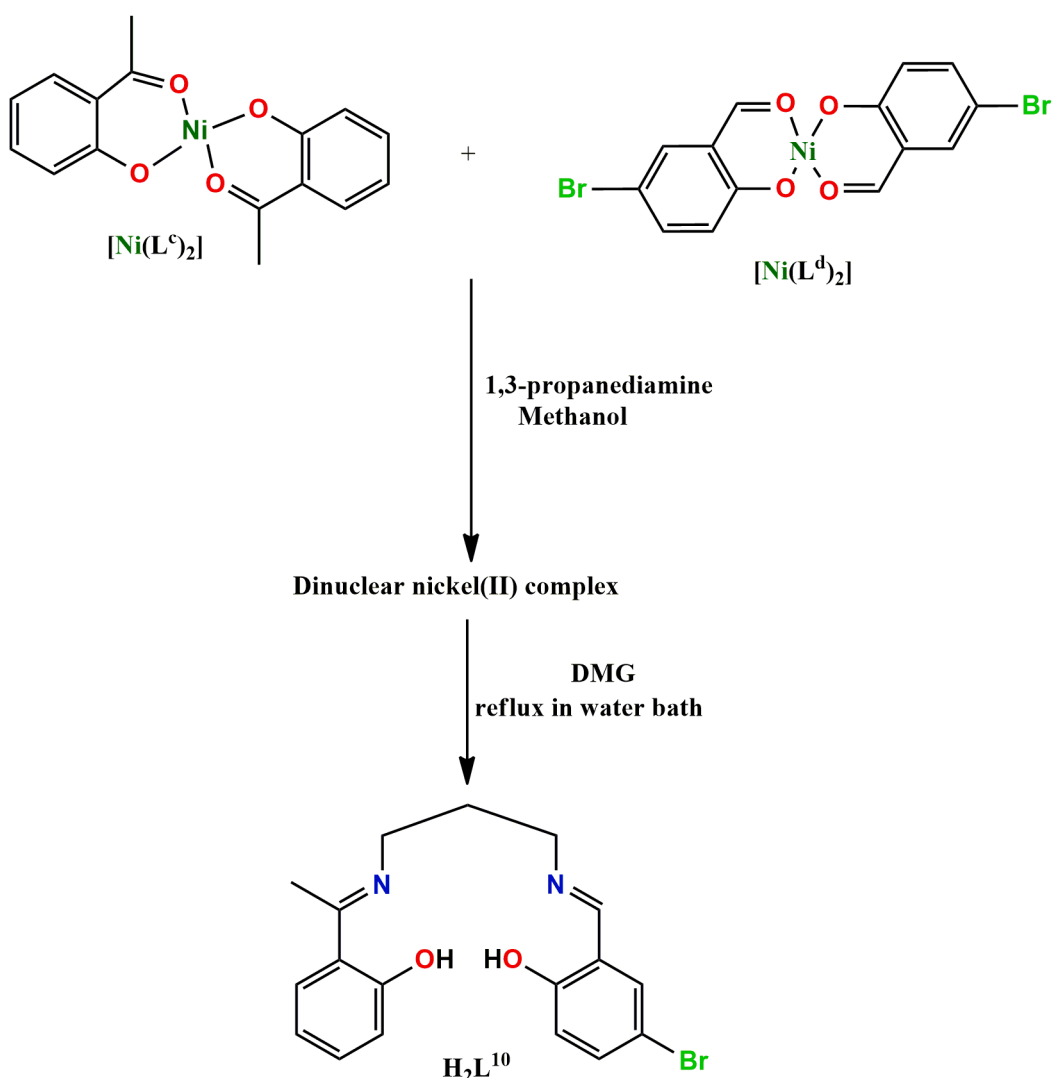
**2.2.3.3.  $[\text{Co}^{\text{II}}\text{L}^{16}]$  (22) and  $[\text{Co}^{\text{III}}\text{L}^{16}(\text{H}_2\text{O})]\text{SbF}_6\cdot 2\text{H}_2\text{O}$  (23).** Cobalt(II) acetate tetrahydrate was added to a yellow solution of  $\text{H}_2\text{L}^{16}$  in diethyl ether under anaerobic conditions to get the red solution of  $[\text{Co}^{\text{II}}\text{L}^{16}]$  (22). The dark red powder was recrystallized by slow evaporation by the solvent.  $[\text{Co}^{\text{III}}\text{L}^{16}(\text{H}_2\text{O})]\text{SbF}_6\cdot 2\text{H}_2\text{O}$  (23) has been prepared as a green product by adding an oxidising agent  $\text{AgSbF}_6$  to a red solution of **22** in DCM under dinitrogen atmosphere at room temperature [48]. The synthetic route of complexes **22** and **23** has been shown in Scheme 34.

#### 2.2.4. Synthesis of manganese(III) complexes

**2.2.4.1.  $[\text{MnL}^{19}\text{Cl}(\text{EtOH})]$  (24).**  $[\text{MnL}^{19}\text{Cl}(\text{EtOH})]$  (24) was prepared by the anhydrous ethanol solution of triethylamine was added in to the hydrothermal reactor with 1:1 M ratio of Schiff base and manganese(II) chloride tetrahydrate then sealed up heated at 80 °C for 3 days to get the complex **24** [49]. The synthetic route of the complex **24** has been shown in Scheme 35.

#### 2.2.5. Synthesis of palladium(II) complexes

**2.2.5.1.  $[\text{PdL}^{15}]$  (25).** A toluene solution of palladium(II) acetate was added to a toluene solution of  $\text{H}_2\text{L}^{15}$  with constant stirring at 100 °C. The reaction mixture was then cooled and left undisturbed in a refrigerator

**Scheme 14.** Synthetic route to  $\text{H}_2\text{L}^{10}$ .

to yield yellow prismatic crystals of  $[\text{PdL}^{15}]$  (25) [43]. It was re-crystallized from hot toluene to get X-ray quality single crystals. The synthetic route of the complex 25 has been shown in Scheme 36.

#### 2.2.6. Synthesis of platinum(II) complexes

**2.2.6.1.  $[\text{PtL}^{14}]\cdot\text{CHCl}_3$  (26).** A DMSO solution of potassium tetrachloroplatinum(II) was added to a DMF solution of  $\text{H}_2\text{L}^{14}$  and sodium acetate with stirring. A small amount of colourless precipitate was filtered off. The filtrate was left undisturbed to get yellow microcrystals of  $[\text{PtL}^{14}]\cdot\text{CHCl}_3$  (26). It was re-crystallized from chloroform to get single crystals, suitable for X-ray diffraction [42]. The synthesis of the complex 26 has been shown in Scheme 37.

**2.2.6.2.  $[\text{PtL}^{15}]$  (27).** A DMSO solution of potassium platinum(II) tetrachloride and sodium acetate was added to a THF solution of  $\text{H}_2\text{L}^{15}$  with constant stirring at 70 °C. A small amount of white precipitate was filtered off. The reaction mixture was left undisturbed in refrigerator to grow yellow prism crystals of  $[\text{PtL}^{15}]$  (27). It was re-crystallized from THF-DMSO system to grow diffraction quality single crystals, suitable for X-ray diffraction [43]. The synthetic route of the complex 27 has been shown in Scheme 38.

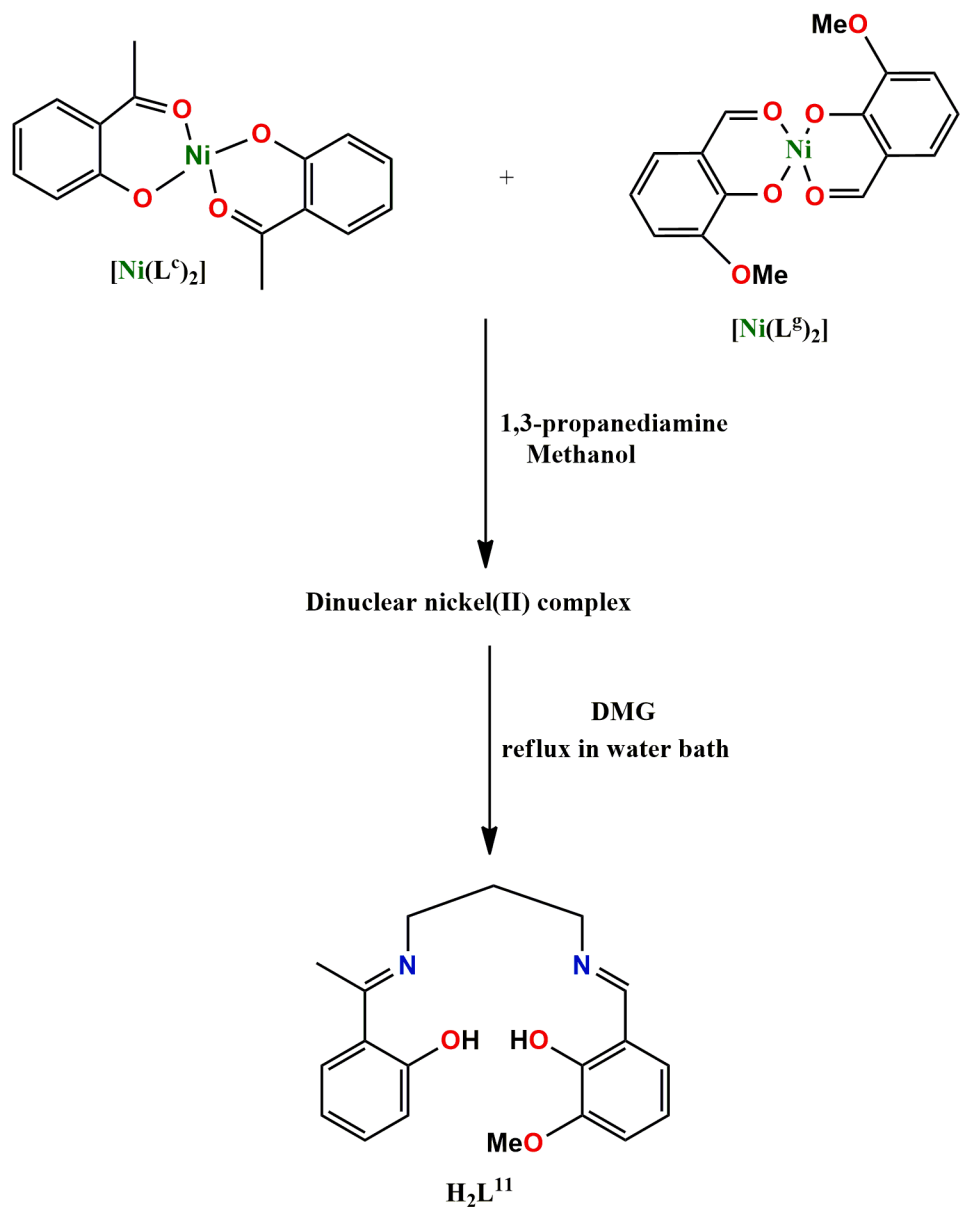
### 3. Structural aspects

The structures of the complexes are retrieved from CCDC. The CCDC numbers and the formulae of the complexes are gathered in Table S1 (Supplementary Information). The structures of the complexes are highlighted below.

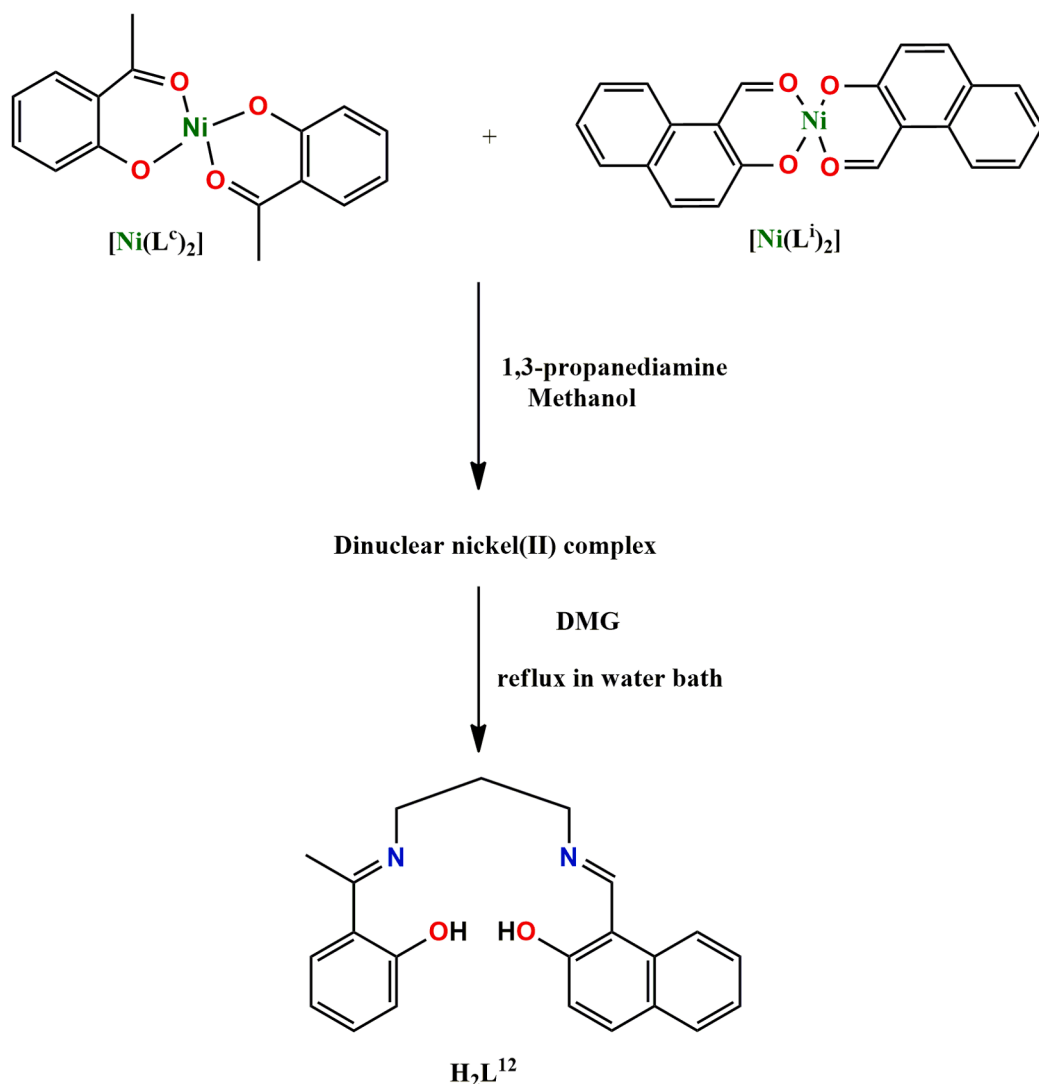
#### 3.1. Copper(II) complexes

##### 3.1.1. $[\text{CuL}^1(\text{H}_2\text{O})]$ (1) and $[\text{CuL}^8(\text{H}_2\text{O})]$ (3)

The central copper(II) is penta-coordinated in each of complexes 1 and 3, and is equatorially coordinated by two imine nitrogen atoms and two phenoxy oxygen atoms of the asymmetric Schiff base ligands,  $\text{H}_2\text{L}^1$  and  $\text{H}_2\text{L}^8$  respectively. One oxygen atom of a water molecule coordinates copper(II) in the apical position to complete the square pyramidal geometry of each complex. Two common geometries of a penta-coordinated complex are trigonal bipyramidal and square pyramidal. In case of complexes 1 and 3, the geometry is best described as square pyramidal. This has been confirmed by the value of the Addison parameter (or trigonality index,  $\tau$ ) [56], which is 0 for complex 1 and 0.05 and 0.07 for two crystallographic ally independent sub-units of complex 3. The Addison parameter is defined as  $(x-y)/60$ , where  $x$  and  $y$  are the largest and 2nd largest L-M-L angles. For a perfectly square pyramid,  $\tau = 0$ , and for a perfectly trigonal bipyramidal,  $\tau = 1$  (Scheme



**Scheme 15.** Synthetic route to  $\text{H}_2\text{L}^{11}$ .



**Scheme 16.** The synthetic route to H<sub>2</sub>L<sup>12</sup>.

39). The apical copper(II)-oxygen distance (2.287(2) Å in 1, and 2.370 (4) Å and 2.358(4) Å in 3) is longer than the equatorial copper(II)-oxygen distances (1.928(2) Å in 1 and 1.934(3) Å, 1.936(3) Å, 1.951 (3) Å and 1.934(3) Å in 3), as expected for copper(II) with d<sup>9</sup> electronic configuration (which is very much susceptible for strong Z-out J.T. distortion) [57].

As expected for a square pyramidal geometry, the copper(II) center is displaced from the mean basal plane passing through two imine nitrogen and two phenoxy oxygen atoms [57]. The deviation of copper(II) from the mean coordinating plane is 0.198 Å. The perspective view of complex 1 is shown in Fig. 1.

### 3.1.2. [CuL<sup>8</sup>(H<sub>2</sub>O)] (3)

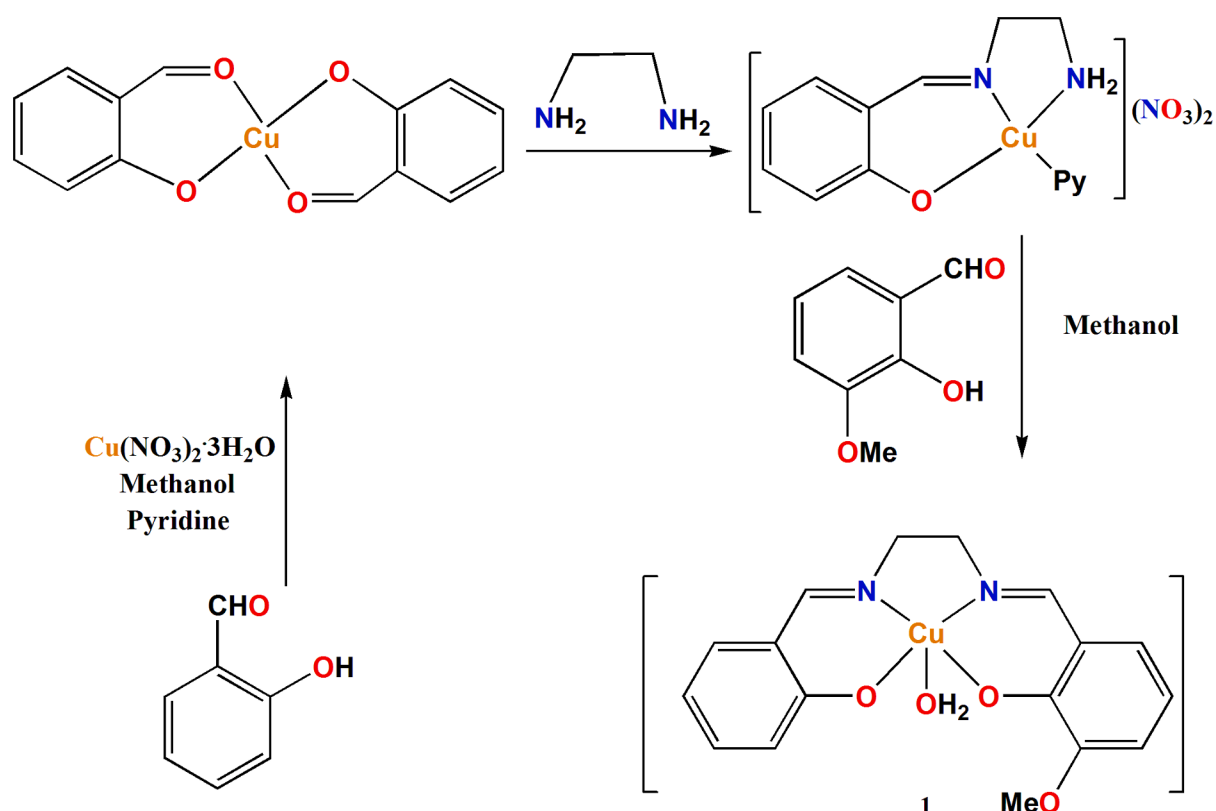
3.1.2.1. [CuL<sup>7</sup>]·3·5H<sub>2</sub>O (2), [CuL<sup>10</sup>]·0·5H<sub>2</sub>O (4), [CuL<sup>11</sup>]·DCM (5), [CuL<sup>12</sup>] (6), [CuL<sup>17</sup>] (7), [CuL<sup>19</sup>]·0·5EtOH·1·25H<sub>2</sub>O (8), [CuL<sup>20</sup>] (9). In each of these complexes, copper(II) center is coordinated by two imine nitrogen atoms and two phenoxy oxygen atoms of the corresponding salen type asymmetric Schiff base to complete the square planar geometry of copper(II). The copper(II)-nitrogen(salen) and copper(II)-oxygen(salen) distances are gathered in Table 2. The deviation of the coordinating atoms from the average plane passing through them and that of the copper(II) from the same plane are gathered in Table 3.

The most common geometry of any tetra-coordinated complex is either square planar or tetrahedral. The exact geometry could be calculated from the  $\tau_4$  index, which is defined as  $\tau_4 = \{360 - (\alpha + \beta)\}/141$ , where  $\alpha$  and  $\beta$  are the two largest angles in the four coordinate species [58]. For a perfectly square planar system,  $\tau_4$  index should be equal to 0. Similarly, for a regular tetrahedral geometry  $\tau_4$  index is very close to 1. The  $\tau_4$  index of tetra-coordinated copper(II) complexes (2–9) are gathered in Table 4. The values indicate that the geometry of each complex is close to square planar. The perspective views of complexes 2–9 are shown in Fig. 2, Fig. 3..

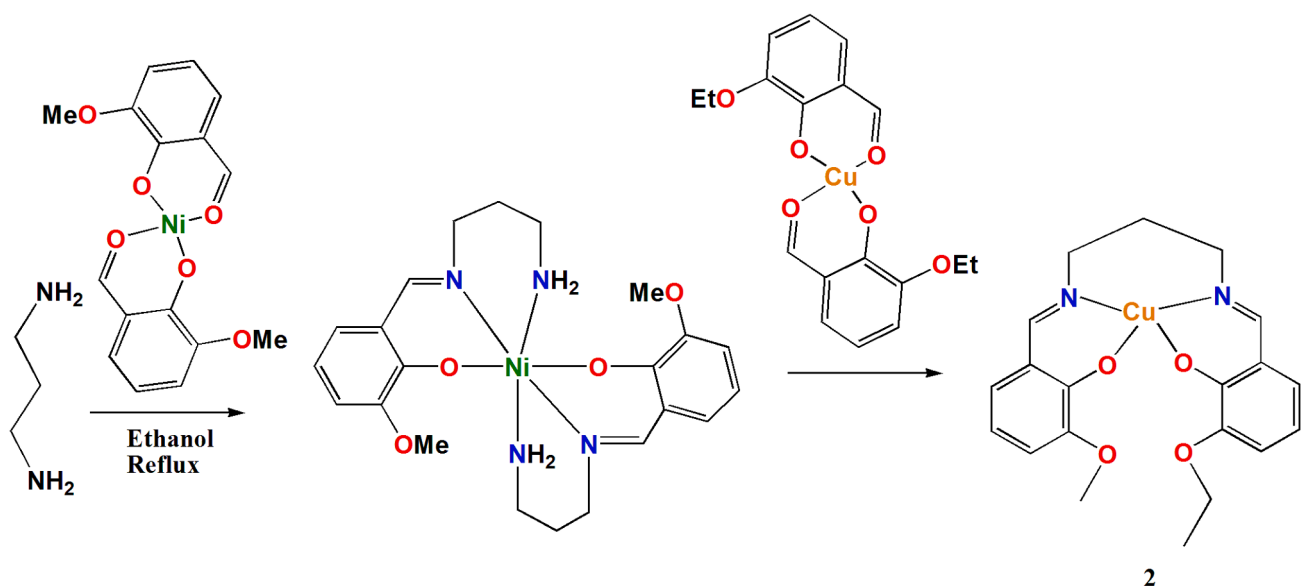
### 3.2. Nickel(II) complexes

#### 3.2.1. [NiL<sup>2</sup>]·0·5H<sub>2</sub>O (10), [NiL<sup>3</sup>]·2H<sub>2</sub>O (11), [NiL<sup>4</sup>]·H<sub>2</sub>O (12), [NiL<sup>6</sup>] (13), [NiL<sup>11</sup>]·DCM (14), [NiL<sup>9</sup>] (15), [NiL<sup>14</sup>]·CHCl<sub>3</sub> (16), [NiL<sup>15</sup>]·CHCl<sub>3</sub> (17), [NiL<sup>16</sup>]·0·39DCM (18) and [NiL<sup>18</sup>] (19).

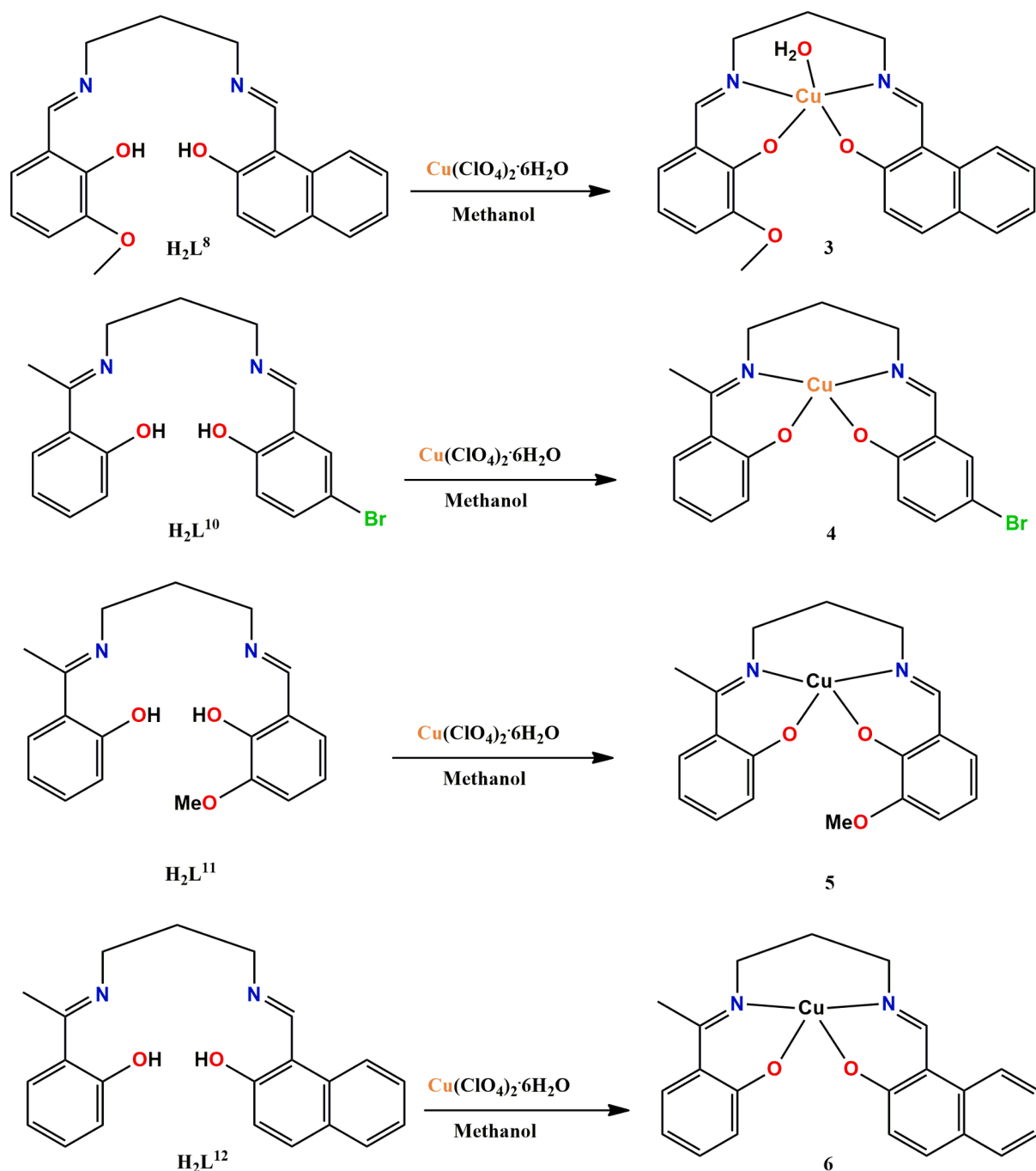
In each of these complexes, the nickel(II) center is showing square planar geometry, being bonded to two imine nitrogen atoms and two phenoxy oxygen atoms of the respective salen type asymmetric Schiff base. Square planar geometry is not uncommon for nickel(II) with d<sup>8</sup> electronic configuration, and tetragonal distortion of octahedral geometry is the driving force for the formation of square planar nickel(II) complexes. The nickel(II)-nitrogen and nickel(II)-oxygen distances are gathered in Table 5. The deviation of the coordinating atoms from the



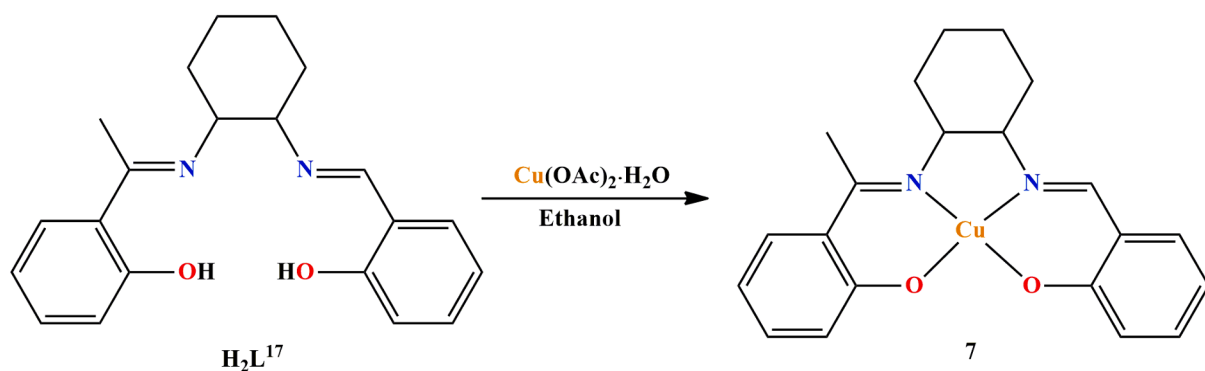
Scheme 17. Synthetic route to complex 1.



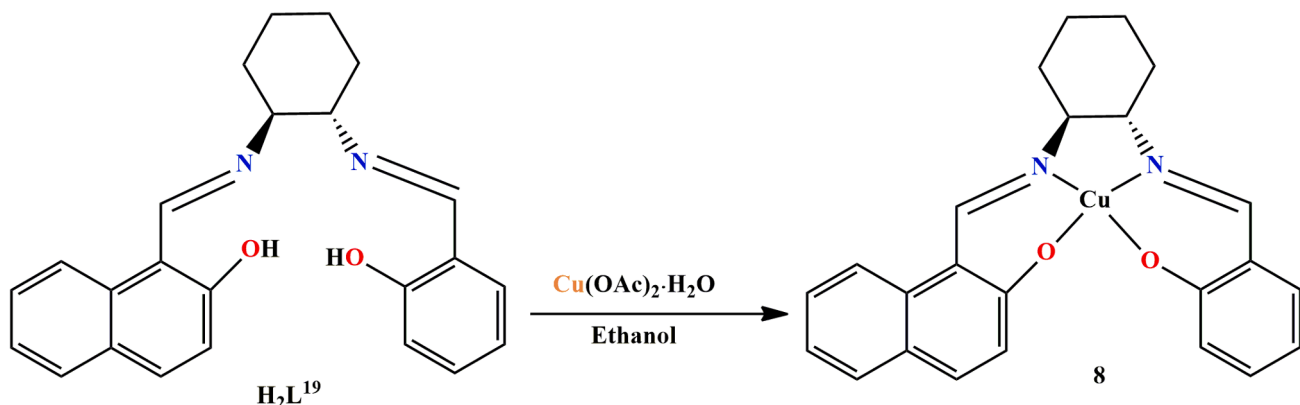
Scheme 18. Synthetic route to complex 2.



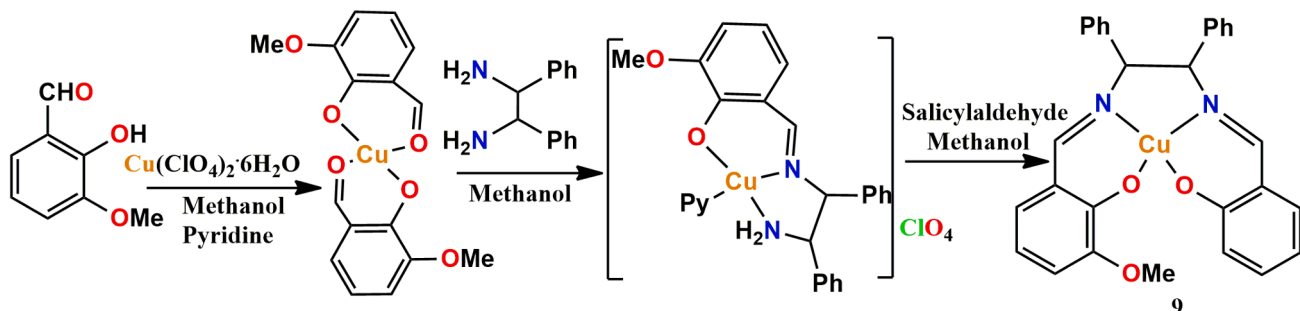
Scheme 19. Synthetic route to complexes 3, 4, 5 and 6.



Scheme 20. The synthetic route to complex 7.



Scheme 21. Synthetic route to complex 8.



Scheme 22. Synthetic route to complex 9.

mean plane passing through them and that of the nickel(II) from the same plane are gathered in Table 3. The  $\tau_4$  index parameter of tetra-coordinated nickel(II) complexes (**10–19**) are gathered in Table 6. The values indicate that the geometry of each complex is close to square planar. The perspective views of the complexes are shown in Figs. 4 and 5.

#### 4. Cobalt complexes

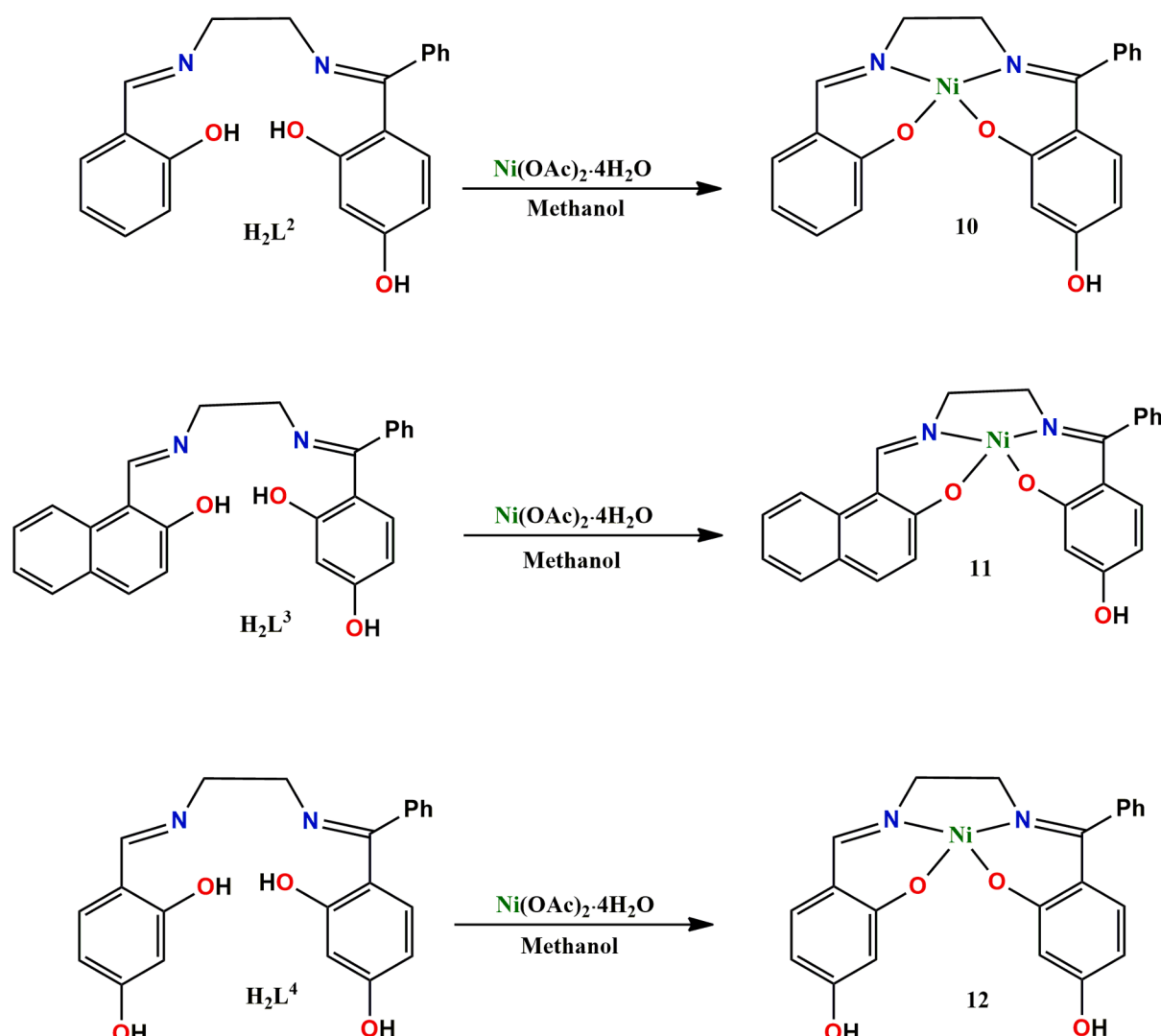
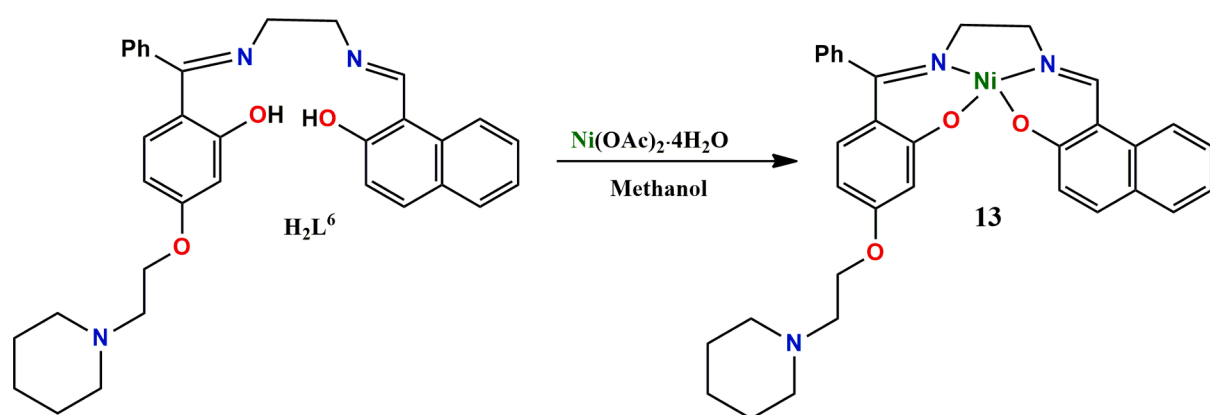
##### 4.1. $[\text{Co}^{\text{III}}\text{L}^5(\text{R},\text{R}-\text{dpen})]\text{Ts}\text{a}\cdot 2\text{EtOH}$ (**20**) [ $\text{dpen} = 1,2$ -diphenylethylenediamine; $\text{HTs}\text{a} = p$ -toluenesulfonic acid]

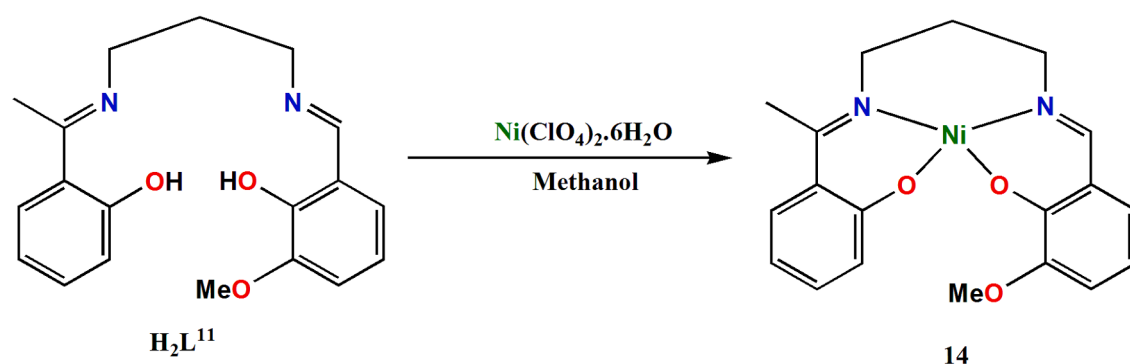
Complex **20** is octahedral, being hexagonally coordinated with two

imine nitrogen atoms and two phenoxy oxygen of the asymmetric di-Schiff base ligand  $\text{H}_2\text{L}^5$ , and fifth and sixth coordinate sites are N(1) and N(2) of 1,2-diphenyl-ethane-1,2-diamine. Perspective view of the complex **20** has been shown in Fig. 6. The cobalt(II)-nitrogen(salen) and cobalt(II)-oxygen(salen) distances in the equatorial plane are gathered in Table 7.

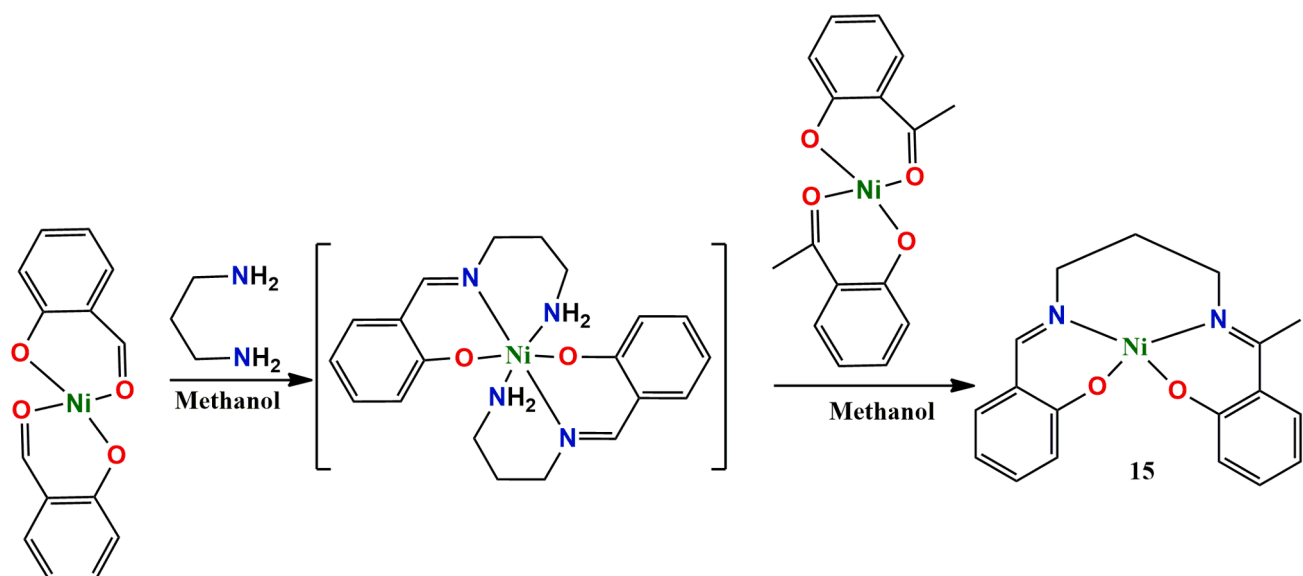
##### 4.2. $[\text{Co}^{\text{II}}\text{L}^{13}]$ (**21**) and $[\text{Co}^{\text{II}}\text{L}^{16}]$ (**22**)

In complexes **21** and **22**, cobalt(II) centers are square planar, being coordinated by two imine nitrogen atoms and two phenoxy oxygen atoms of the respective tetra-dentate asymmetric Schiff bases,  $\text{H}_2\text{L}^{13}$  and  $\text{H}_2\text{L}^{16}$ . Cobalt(II) is  $d^7$  and square planar geometry is not so common for

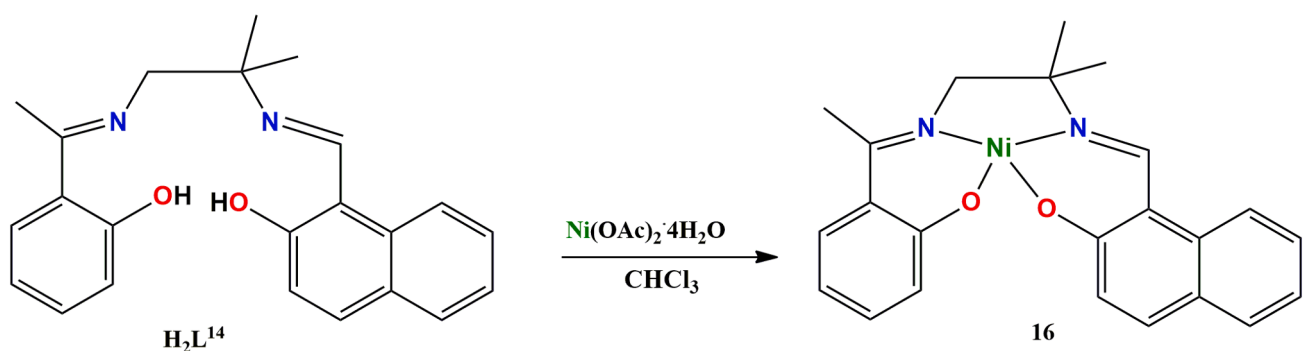
Scheme 23. The synthetic routes to complexes **10–12**.Scheme 24. Synthesis route to complex **13**.



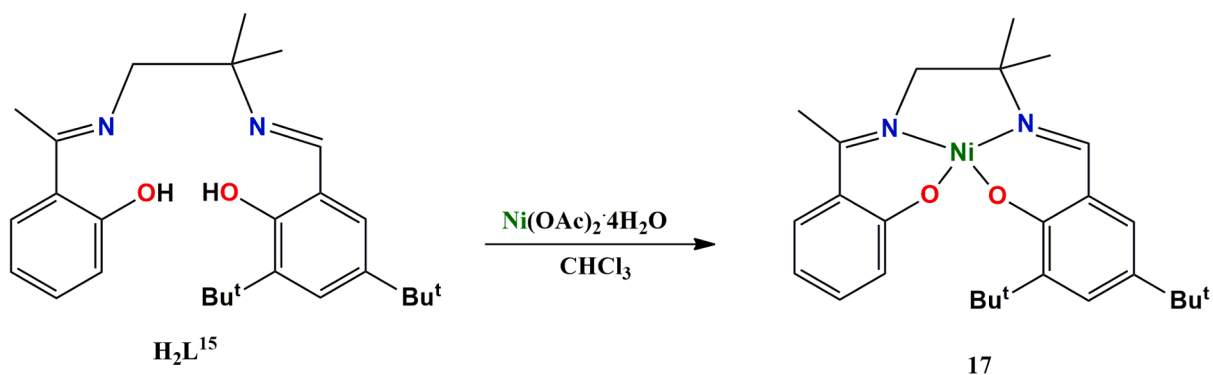
Scheme 25. Synthesis route to complex 14.



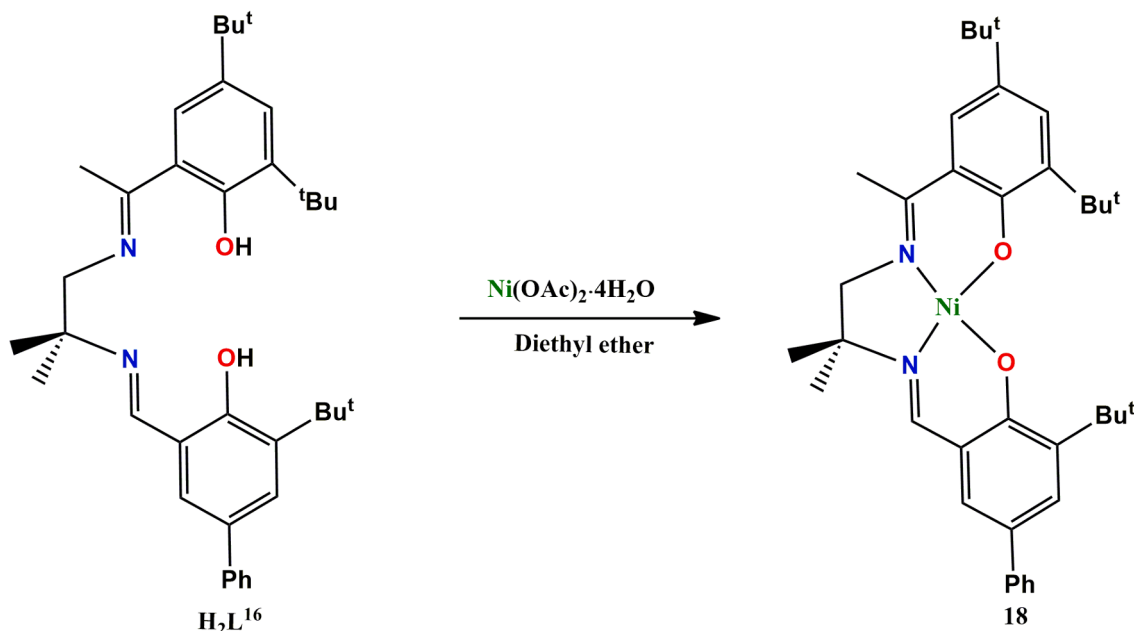
Scheme 27. The synthetic route to complex 15.



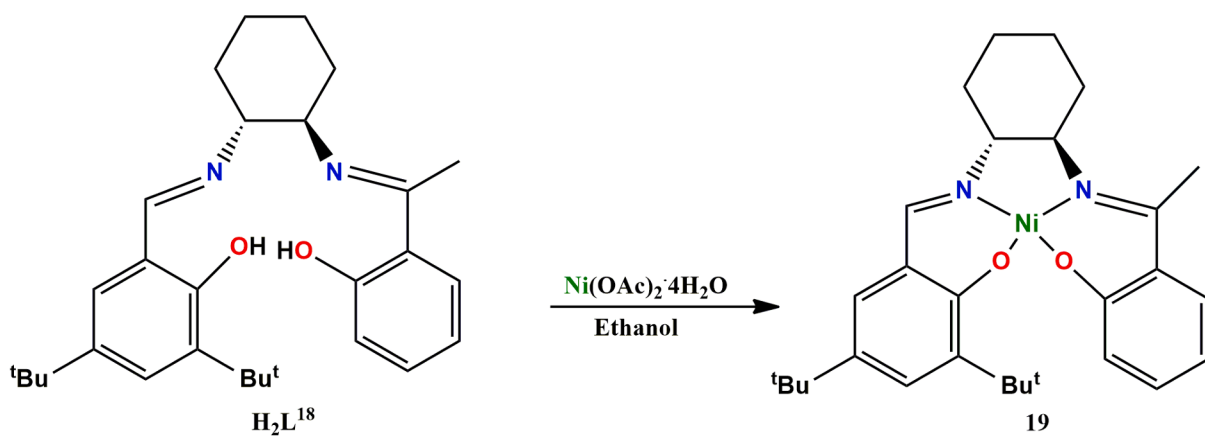
Scheme 28. The synthesis route to complex 16.



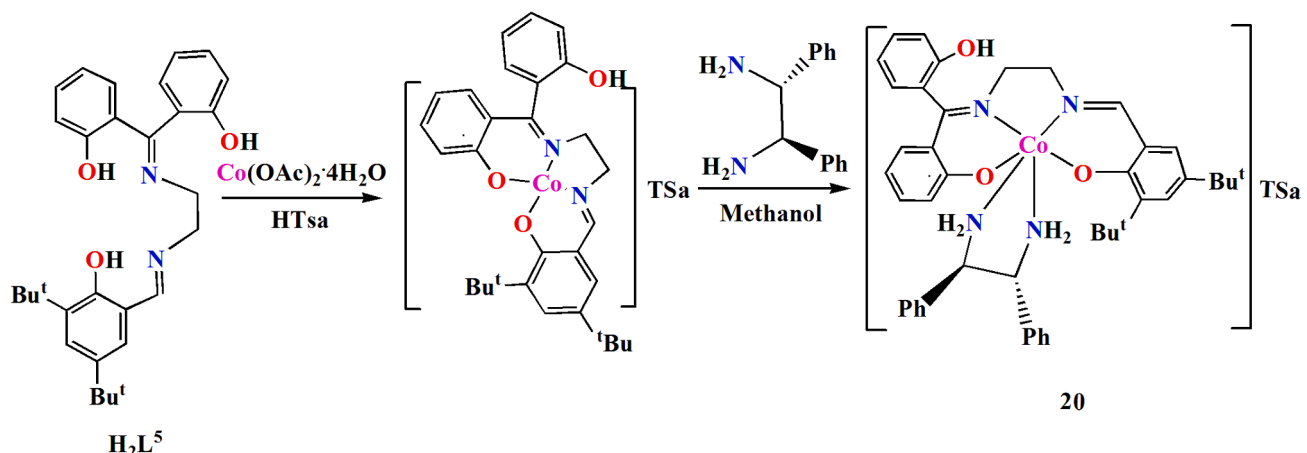
**Scheme 29.** Synthesis route to complex 17.



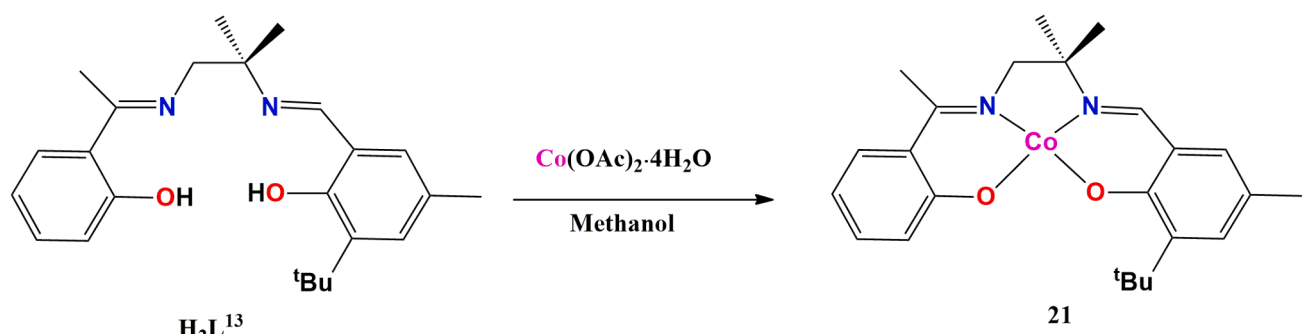
**Scheme 30.** Synthesis route to complex **18**.



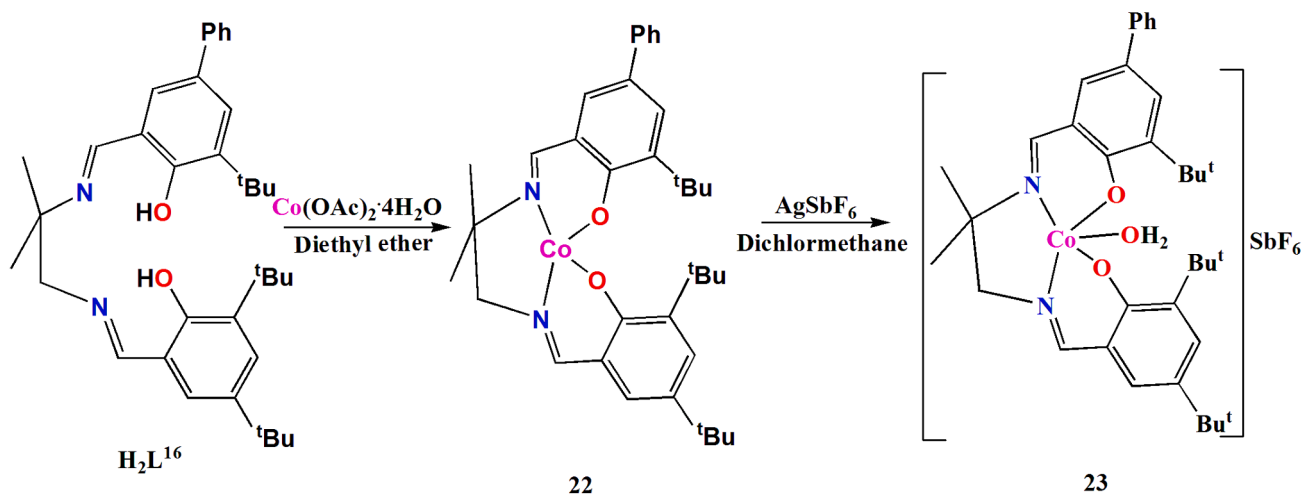
**Scheme 31.** Synthesis route to complex **19**.



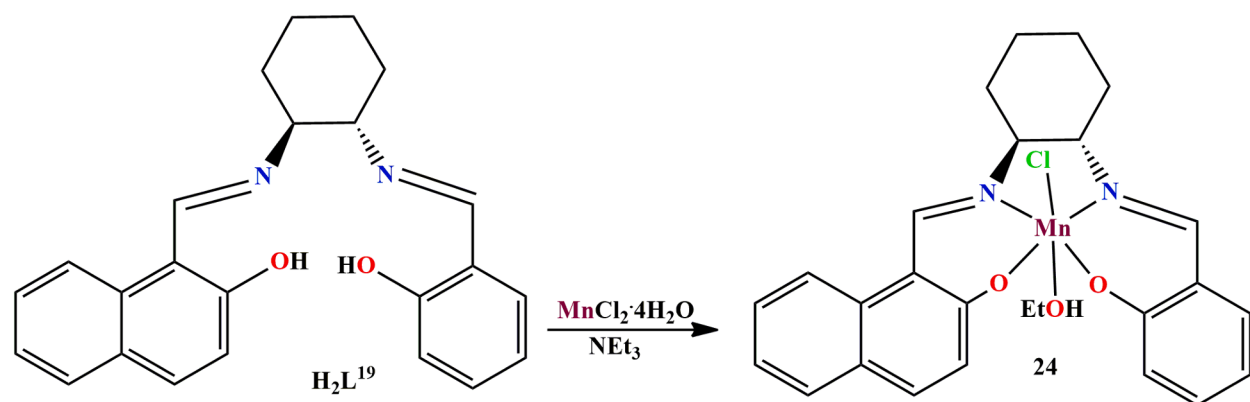
Scheme 32. Synthetic route to complex 20.



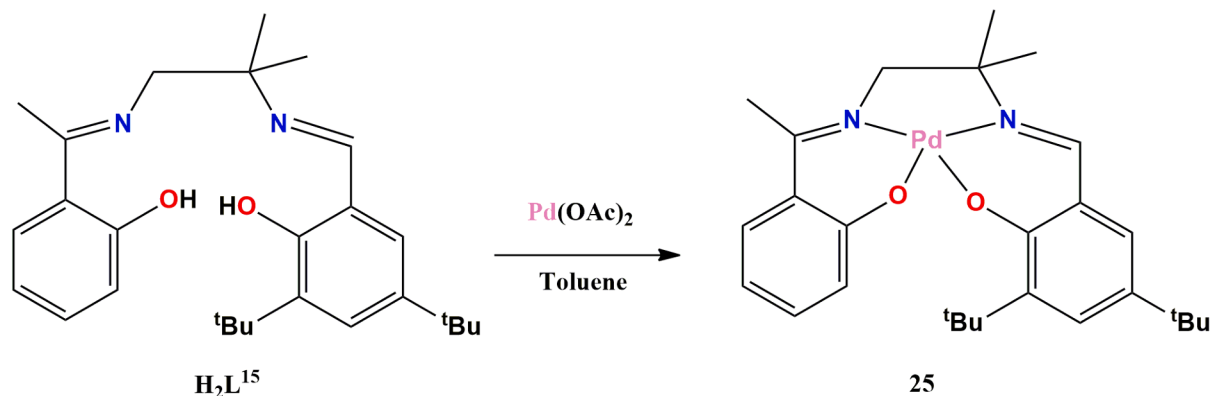
Scheme 33. Synthetic route to complex 21.



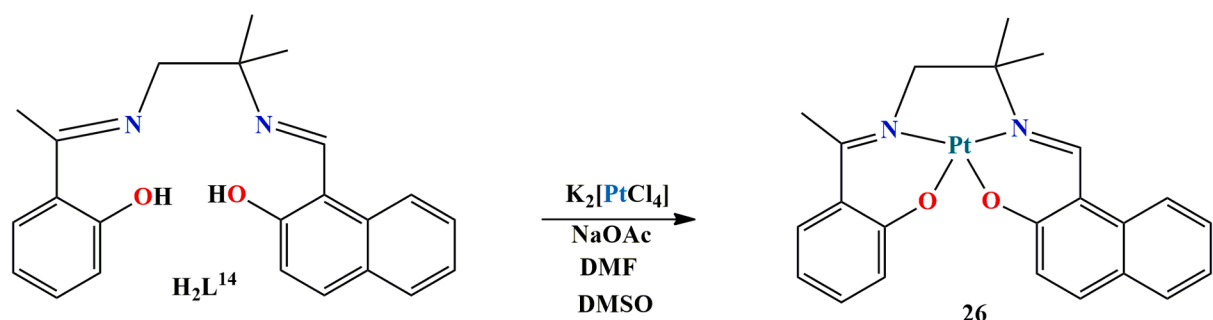
Scheme 34. Synthetic route to complexes 22 and 23.



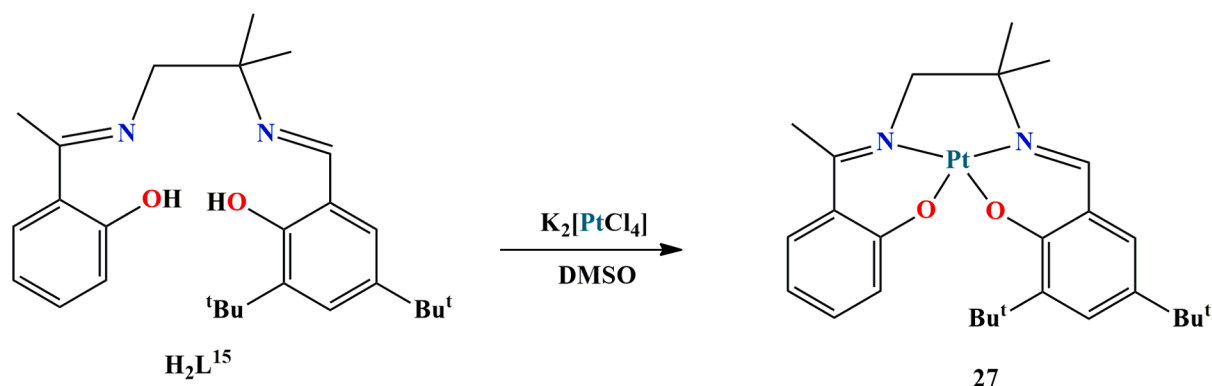
Scheme 35. Synthetic route to complex 24.



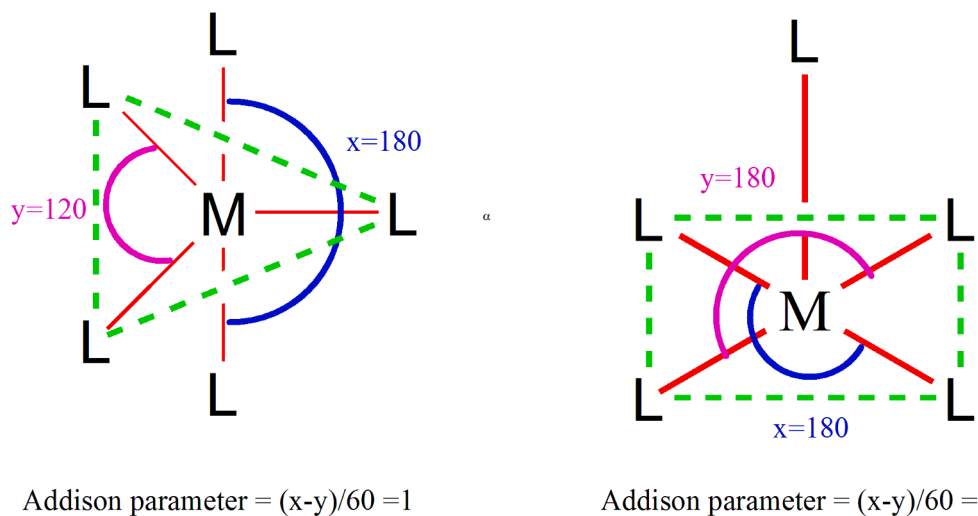
Scheme 36. The synthetic route of complex 25.



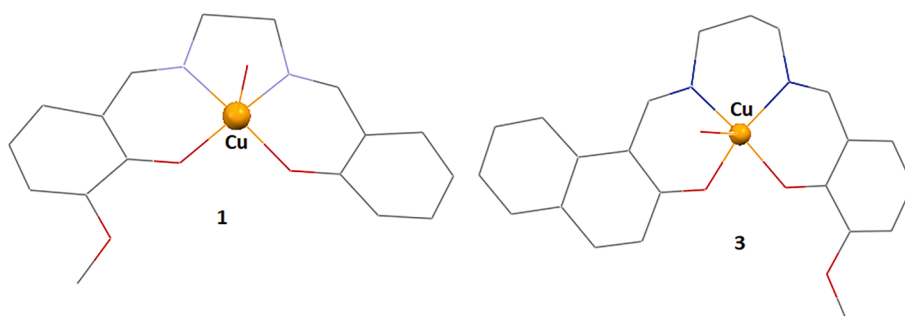
Scheme 37. The synthetic route to complex 26.



Scheme 38. Synthesis route to complex 27.



Scheme 39. Schematic representation of TBP and square pyramidal geometry; and calculation of their Addison parameter values.

Fig. 1. Perspective view of complex  $[\text{CuL}^1(\text{H}_2\text{O})]$  (1) and  $[\text{CuL}^8(\text{H}_2\text{O})]$  (3). Hydrogen atoms have been omitted for clarity.

cobalt(II). The cobalt(II)-nitrogen(imine) and cobalt(II)-oxygen(imine) distances are gathered in Table 7. The deviation of the coordinating atoms from the mean plane passing through them and that of the cobalt (II) from the same plane are gathered in Table 3. The  $\tau_4$  index of tetra-coordinated cobalt(II) complexes are gathered in Table 8.

The perspective views of the complexes are shown in Fig. 7. The  $\tau_4$  index parameters of the complexes (21–22) are gathered in Table 8. The values indicate that the geometry of each complex is essentially square planar. It is interesting to note that in the solid state structure of 21, a supra-molecular dimer (Fig. 8) has been stabilized by C—H—pi interaction, in which cobalt(II)—cobalt(II) distance is relatively small (3.88 Å).

#### 4.3. $[\text{Co}^{\text{III}}\text{L}^{16}(\text{H}_2\text{O})]\text{SbF}_6 \cdot 2\text{H}_2\text{O}$ (23)

In complex 23, the central penta-coordinated cobalt(III) is equatorially coordinated by two imine nitrogen atoms and two phenoxy oxygen atoms of the asymmetric Schiff base ligand,  $\text{H}_2\text{L}^{16}$ . One oxygen atom of a water molecule coordinates copper(II) in the apical position to complete its square pyramidal geometry. The Addison parameter of this complex is 0.03, which confirms the distorted square pyramidal geometry. The cobalt(III)-nitrogen(imine) and cobalt(III)-oxygen(imine) distances are gathered in Table 7. The apical cobalt(III)-oxygen distance (2.124(4) Å) is longer than the equatorial cobalt(III)-oxygen distances (1.846(3)-1.868(4) Å).

**Table 2**

The M- O<sub>phenoxo</sub> and M- N<sub>imine</sub> bond lengths (involving the salen type Schiff bases) in complexes **1–9**.

Complexes	M-N <sub>imine</sub> (Å)	Cu(II)-O <sub>imine</sub> (Å)	Ref
[CuL <sup>1</sup> (H <sub>2</sub> O)] ( <b>1</b> )	1.950(2)	1.928(2)	33
[CuL <sup>7</sup> ]·3·5H <sub>2</sub> O ( <b>2</b> )	1.983(7), 1.968(7)	1.921(5), 1.925(5)	34
[CuL <sup>8</sup> (H <sub>2</sub> O)] ( <b>3</b> )	1.996(5), 1.977(4)	1.934(3), 1.936(3)	35
[CuL <sup>10</sup> ]·0.5H <sub>2</sub> O ( <b>4</b> )	1.970(4), 1.950(4)	1.879(3), 1.915(4)	35
[CuL <sup>11</sup> ]·DCM( <b>5</b> )	1.956(2), 1.951(2)	1.892(2), 1.901(2)	35
[CuL <sup>12</sup> ] ( <b>6</b> )	1.997(3), 1.948(2)	1.894(2), 1.923(2)	35
[CuL <sup>17</sup> ] ( <b>7</b> )	1.921(3), 1.972(2)	1.903(2), 1.870(3)	36
[CuL <sup>19</sup> ]·0.5EtOH·1.25H <sub>2</sub> O ( <b>8</b> )	1.942(8), 1.919(5)	1.898(7), 1.910(8)	36
[CuL <sup>20</sup> ] ( <b>9</b> )	1.951(4), 1.944(4)	1.914(3), 1.902(4)	36

As expected for a square pyramidal geometry, the cobalt(III) center is displaced from the mean basal plane passing through two imine nitrogen and two phenoxy oxygen atoms. The deviation of cobalt(III) from this mean coordinating plane is 0.147 Å towards the direction of apical water molecule. The perspective view of complex **23** has been shown in Fig. 9.

#### 4.4. [MnL<sup>19</sup>Cl(EtOH)] (**24**)

The manganese(III) is octahedral being bonded to two phenoxy oxygen atoms and two imine nitrogen atoms of the dianion of the tetradentate asymmetric Schiff base, H<sub>2</sub>L<sup>19</sup> in the equatorial plane. The axial positions are occupied by one chlorine atom and an oxygen atom from an ethanol molecule. Mn(III) is a Jahn-Teller ion with d<sup>4</sup> (t<sub>2g</sub><sup>3</sup>e<sub>g</sub><sup>1</sup>) electronic configuration and consequently, the axial Mn(III)-ligand

**Table 3**

The deviation of the coordinating atoms of salen type Schiff base from the average equatorial plane passing through them and that of the metal ion from the same plane in the square planar complexes.

Complexes	Deviation of N <sub>imine</sub> (Å)	Deviation of O <sub>imine</sub> (Å)	Deviation of metal ions (Å)	Ref
2	0.350, 0.351, 0.343, 0.340, 0.218, 0.222	0.399, 0.398, 0.385, 0.381, 0.243, 0.014	0.029, 0.044, 0.014	34
4	0.070, 0.068	0.078, 0.080	0.039	35
5	0.320, 0.309	0.321, 0.332	0.047	35
6	0.040	0.045	0.029	35
7	0.219, 0.222	0.215, 0.217	0.032	36
8	0.071, 0.070, 0.162, 0.166	0.069, 0.068, 0.155, 0.160	0.005, 0.015	37
9	0.167, 0.166	0.161, 0.162	0.008	36
10	0.037	0.039	0.045	39
11	0.020	0.020	0.006	39
12	0.053, 0.054	0.055, 0.056	0.033	39
13	0.075, 0.074, 0.063	0.077, 0.076, 0.065	0.011, 0.020	39
14	0.295, 0.284	0.298, 0.309	0.037	40
15	0.056	0.064, 0.065	0.024	41
16	0.036	0.037, 0.038	0.014	42
17	0.047, 0.048	0.049, 0.050	0.002	43
18	0.059	0.059, 0.060	0.029	44
19	0.052, 0.050	0.054, 0.052	0.020	45
21	0.039	0.041	0.004	47
22	0.107, 0.106	0.106, 0.105	0.025	48
25	0.044	0.043, 0.042	0.013	43
26	0.025	0.024	0.031	42
27	0.026	0.025	0.012	43

**Table 4**

The  $\tau_4$  index of tetra-coordinated copper(II) complexes.

Complexes	Largest L-M-L angles (°)	2nd largest L-M-L angles (°)	$\tau_4$ index	Ref
2	158.9(2)	155.4(2)	0.32	34
4	175.26(16)	170.34(15)	0.10	35
5	163.57(8)	157.92(8)	0.27	35
6	175.65(9)	172.72(9)	0.08	35
7	168.45(18)	164.83(19)	0.19	36
8	175.2(3)	175.0(4)	0.07	37
9	170.22(16)	169.37(16)	0.14	38

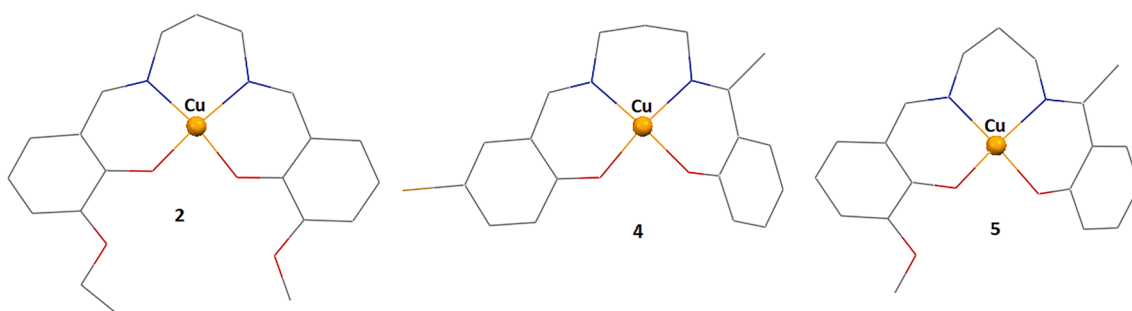


**Fig. 2.** Perspective views of complexes [CuL<sup>7</sup>]·3·5H<sub>2</sub>O (**2**), [CuL<sup>10</sup>]·0·5H<sub>2</sub>O (**4**), [CuL<sup>11</sup>]·DCM (**5**). Hydrogen atoms and lattice solvent molecules have been omitted for clarity.

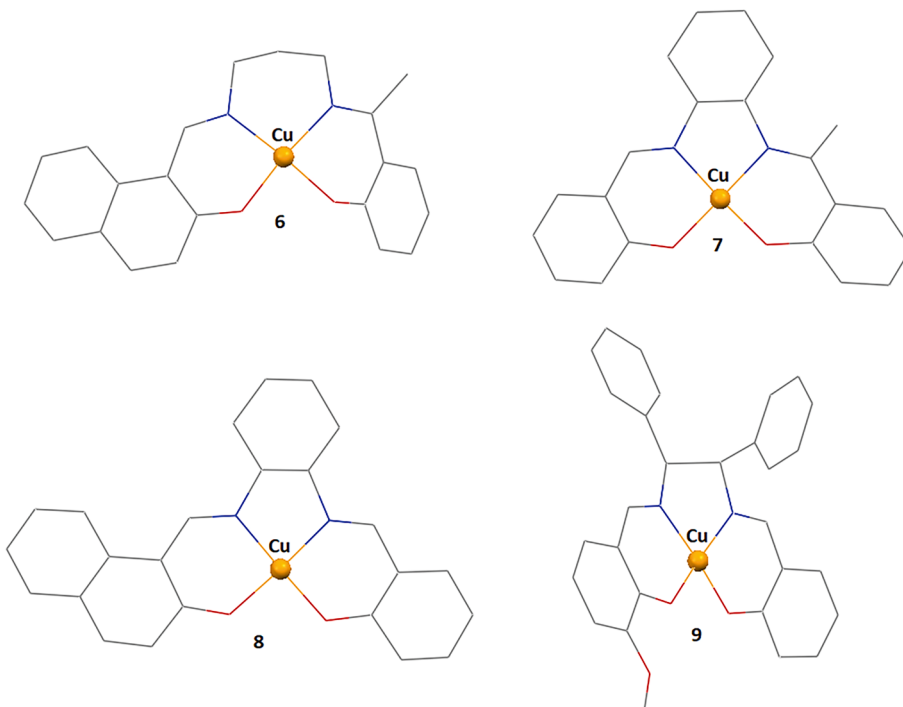


**Fig. 3.** Perspective views of complexes  $[\text{CuL}^{12}]$  (6),  $[\text{CuL}^{17}]$  (7),  $[\text{CuL}^{19}]\text{-}0.5\text{EtOH}\text{-}1.25\text{H}_2\text{O}$  (8),  $[\text{CuL}^{20}]$  (9). Hydrogen atoms and lattice solvent molecules have been omitted for clarity.

**Table 5**

The nickel(II)-O<sub>phenoxo</sub> and nickel(II)-N<sub>imine</sub> bond lengths (involving the salen type Schiff bases) in complexes 10–19.

Formula of the complexes	Ni(II)-N <sub>imine</sub> (Å)	Ni(II)-O <sub>imine</sub> (Å)	Ref
$[\text{NiL}^2]\text{-}0.5\text{H}_2\text{O}$ (10)	1.863(1), 1.838(2)	1.841(1), 1.839(1)	39
$[\text{NiL}^3]\text{-}2\text{H}_2\text{O}$ (11)	1.840(2), 1.860(2)	1.854(1), 1.831(1)	39
$[\text{NiL}^4]\text{-H}_2\text{O}$ (12)	1.871(2), 1.834(2)	1.836(2), 1.848(2)	39
$[\text{NiL}^6]$ (13)	1.865(2), 1.847(2)	1.838(2), 1.856(2)	39
$[\text{NiL}^{11}]\text{-DCM}$ (14)	1.939(3), 1.934(3)	1.886(2), 1.886(3)	40
$[\text{NiL}^7]$ (15)	1.920(2), 1.970(2)	1.888(2), 1.873(2)	41
$[\text{NiL}^{14}]\text{-CHCl}_3$ (16)	1.845(4), 1.852(4)	1.841(3), 1.832(4)	42
$[\text{NiL}^{15}]\text{-CHCl}_3$ (17)	1.853(2), 1.869(2)	1.845(1), 1.837(1)	43
$[\text{NiL}^{16}]\text{-}0.39\text{DCM}$ (18)	1.857(4), 1.849(3)	1.841(2), 1.875(3)	44
$[\text{NiL}^{18}]$ (19)	1.806(3), 1.876(4)	1.839(2), 1.808(3)	45

**Table 6**

The  $\tau_4$  index of tetra-coordinated nickel(II) complexes, 10–19.

Complexes	Largest L-M-L angles (°)	2nd largest L-M-L angles (°)	$\tau_4$ index	Ref
10	178.22(7)	174.51(7)	0.05	39
11	178.22(8)	178.07(8)	0.03	39
12	178.65(9)	174.12(9)	0.04	39
13	175.63(9)	174.68(9)	0.07	39
14	164.37(13)	159.66(13)	0.26	40
15	172.84(9)	172.54(9)	0.10	41
16	177.30(17)	176.41(16)	0.04	42
17	176.98(6)	176.10(6)	0.05	43
18	178.07(13)	174.53(14)	0.05	44
19	176.66(15)	175.55(16)	0.06	45

distances ( $\text{Mn(III)}\text{-Cl}$ , 2.566(1) Å;  $\text{Mn(III)}\text{-O}$ , 2.464(2) Å) are much longer compared to equatorial Mn(III)-lignad distances (1.8–2.0 Å). In the equatorial plane, manganese(III)-O<sub>imine</sub> distance (1.877(2) Å) is slightly shorter than manganese(III)-N<sub>imine</sub> distances (1.991(2) Å, 1.979 (2) Å). The distances are similar to those observed in other manganese(III) complexes with symmetrical tetra-dentate Schiff base ligands [49]. The perspective view of the complex 24 has been shown in Fig. 10.

#### 4.5. Palladium(II) and Platinum(II) complexes, $[\text{PdL}^{15}]$ (25), $[\text{PtL}^{14}]\text{-CHCl}_3$ (26) and $[\text{PtL}^{15}]$ (27)

In complexes 25, 26 and 27, palladium(II) and platinum(II) centers are square planar, as expected for any palladium(II) and platinum(II) complexes. The palladium(II) and platinum(II) centers are coordinated by two imine nitrogen atoms and two phenoxo oxygen atoms of the respective tetra-dentate asymmetric Schiff bases ( $\text{H}_2\text{L}^{15}$  or  $\text{H}_2\text{L}^{14}$ ). The deviation of the coordinating atoms from the mean plane passing through them and that of palladium(II) or platinum(II) from the same plane are gathered in Table 3. The perspective views of the complexes are shown in Fig. 11. The platinum(II)/palladium(II)-nitrogen and platinum(II)/palladium(II)-oxygen distances are gathered in Table 9. The  $\tau_4$  index parameters of the complexes (25–27) are gathered in Table 10. The deviation of the coordinating atoms from the average plane passing through them and that of the palladium(II)/platinum(II) from the same plane are gathered in Table 3.

#### 5. Spectral and magnetic characterization

The IR spectra of the complexes show two strong peaks in the range 1500–1650 cm<sup>-1</sup> due to two types of azomethine (C=N) stretching of the unsymmetrical Schiff bases [33–49]. The frequencies of C=N stretching vibrations are somewhat lowered (~20 cm<sup>-1</sup>) than that observed in free ligands on coordination to the metal centres. The red shift of this C=N absorption on going from the free ligands to the complexes indicates the weak  $\pi$ -accepting behaviour of the chelated ligand (vide infra). In case of IR spectroscopy, the direction of the shift of the bands depends on the nature of the metal and ligands. For example, metal Schiff base complexes display IR absorption bands for imine bond (C=N) at lower wavenumber than the free Schiff bases. The imine functionality (C=N) of the Schiff base coordinates metals synergistically ( $\sigma$ -donation and  $\pi$ -back donation). To be specific, imine (C=N) donates its electron pair (i.e. the lone pair on nitrogen) to metal from a non-bonding type of molecular orbitals (HOMO), and accepts electrons in its vacant antibonding type molecular orbital (LUMO) from the filled d<sub>π</sub>-

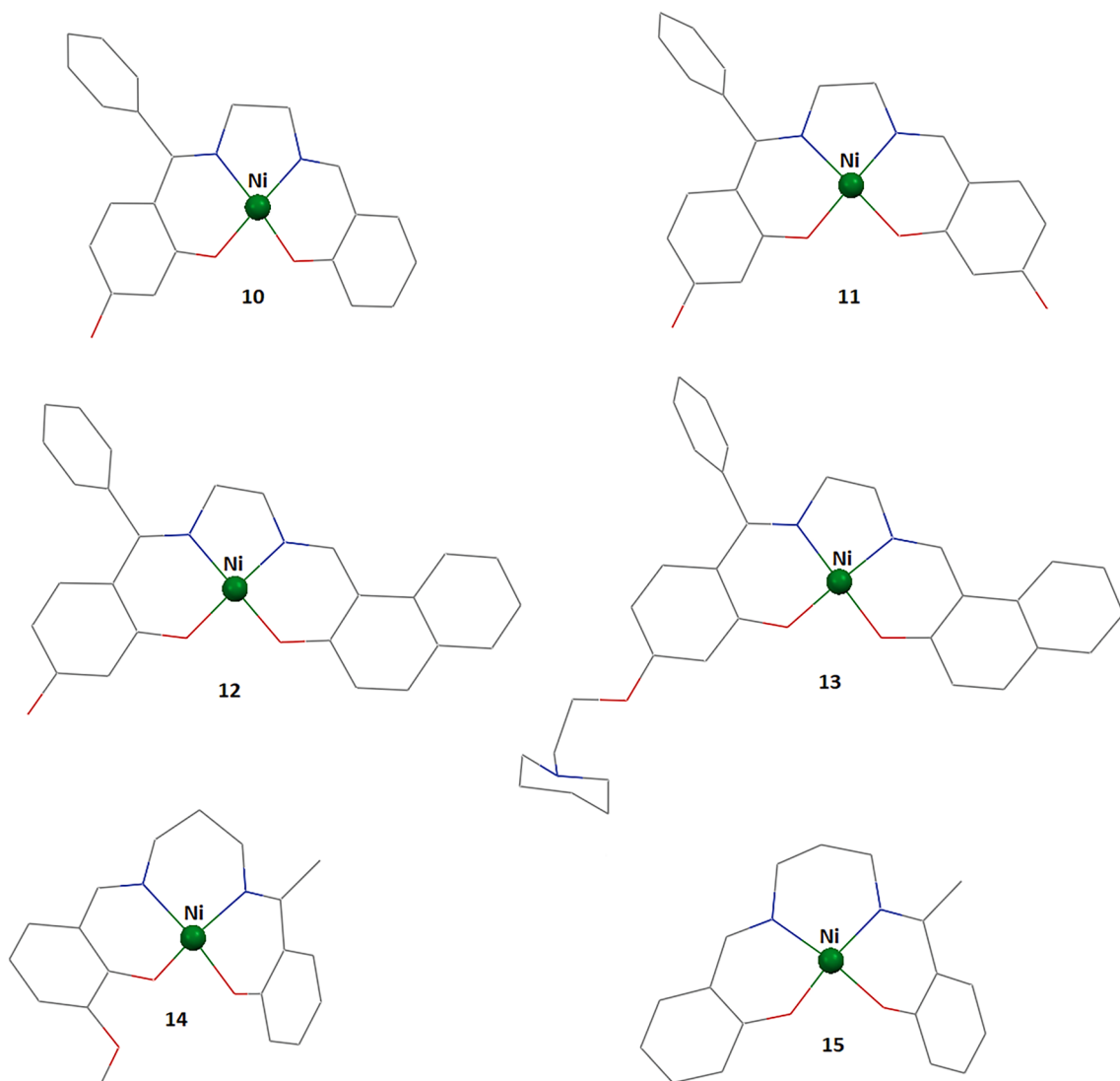


**Fig. 4.** Perspective view of complexes  $[\text{NiL}^2] \cdot 0.5\text{H}_2\text{O}$  (10),  $[\text{NiL}^3] \cdot 2\text{H}_2\text{O}$  (11),  $[\text{NiL}^4] \cdot \text{H}_2\text{O}$  (12),  $[\text{NiL}^6]$  (13),  $[\text{NiL}^{11}] \cdot \text{DCM}$  (14),  $[\text{NiL}^9]$  (15). Hydrogen atoms and lattice solvent molecules have been omitted for clarity.

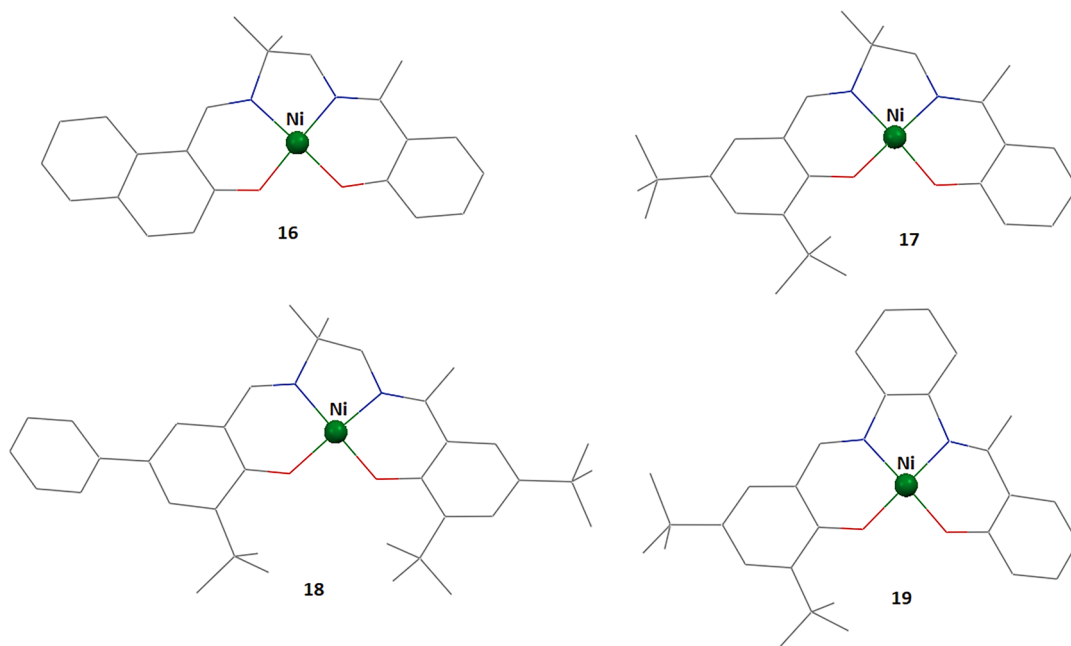


**Fig. 5.** The perspective view of complexes  $[\text{NiL}^{14}] \cdot \text{CHCl}_3$  (**16**),  $[\text{NiL}^{15}] \cdot \text{CHCl}_3$  (**17**),  $[\text{NiL}^{16}] \cdot 0.39\text{DCM}$  (**18**) and  $[\text{NiL}^{18}]$  (**19**). Hydrogen atoms and lattice solvent molecules have been omitted for clarity.

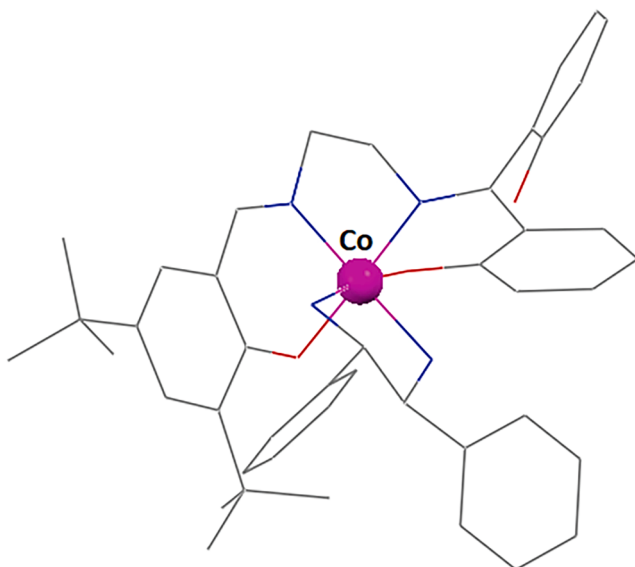


**Fig. 6.** Perspective view of complex **20**. Hydrogen atoms, lattice ethanol molecules and counter anion have been omitted for clarity.

**Table 7**

The  $\text{M}-\text{O}_{\text{phenoxo}}$  and  $\text{M}-\text{N}_{\text{imine}}$  bond lengths (involving the salen type Schiff bases) in complexes **20–23**. M = cobalt(III) in complexes **20** and **23**, M = cobalt(II) in complexes **21** and **22**.

Complexes	$\text{M}-\text{N}_{\text{imine}} (\text{\AA})$	$\text{M}-\text{O}_{\text{imine}} (\text{\AA})$	Ref
$[\text{Co}^{\text{III}}\text{L}^5(\text{R},\text{R-dpen})]\text{Tsa}\cdot 2\text{EtOH}$ ( <b>20</b> )*	1.874(2), 1.890(3)	1.888(2), 1.881(2)	<a href="#">46</a>
$[\text{Co}^{\text{II}}\text{L}^{19}]$ ( <b>21</b> )	1.874(1), 1.857(2)	1.823(1), 1.838(1)	<a href="#">47</a>
$[\text{Co}^{\text{II}}\text{L}^{16}]$ ( <b>22</b> )	1.872(2), 1.860(2)	1.835(2), 1.875(2)	<a href="#">48</a>
$[\text{Co}^{\text{III}}\text{L}^{16}(\text{H}_2\text{O})]\text{SbF}_6\cdot 2\text{H}_2\text{O}$ ( <b>23</b> )	1.891(4), 1.892(4)	1.868(4), 1.846(3)	<a href="#">48</a>

\* [dpen = 1,2-diphenylethylenediamine; HTsa = Toluenesulfonic acid].

**Table 8**  
The  $\tau_4$  index of tetra-coordinated cobalt(II) complexes, **21** and **22**.

Complexes	Largest L-M-L angles ( $^\circ$ )	2nd largest L-M-L angles ( $^\circ$ )	$\tau_4$ index	Ref
<b>21</b>	177.36(7)	177.18(6)	0.04	<a href="#">47</a>
<b>22</b>	174.88(9)	171.99(9)	0.09	<a href="#">48</a>

orbitals of metal. However, both  $\sigma$ -donation and  $\pi$ -acceptance result a decrease in the C=N bond order, which is consistent with the IR absorption band at relatively lower frequency.

The mono-nuclear copper(II) complexes (**1–9**) are expected to have magnetic moments close to  $1.73 \mu\text{B}$ , as they have only one unpaired electron. Unfortunately the magnetic moments were not measured and reported in literature [33–48]. The square planar nickel(II), palladium(II) and platinum(II) complexes (**10–19**, **25**, **26** and **27**) are essentially diamagnetic, as expected for such systems with no unpaired electrons [39–45]. The magnetic moments of cobalt(II) complexes **21** and **22** are close to  $\sim 1.73 \mu\text{B}$  ( $2.02 \mu\text{B}$  for **21** and  $1.75 \mu\text{B}$  for **22**), which are typical for square planar low spin  $d^7$  systems ( $S = 1/2$ ) [47,48]. Cobalt(III) complexes (**20**, **23**) are again diamagnetic as expected for their low spin  $t_{2g}^6$  electronic configurations with no unpaired electrons [46,48].

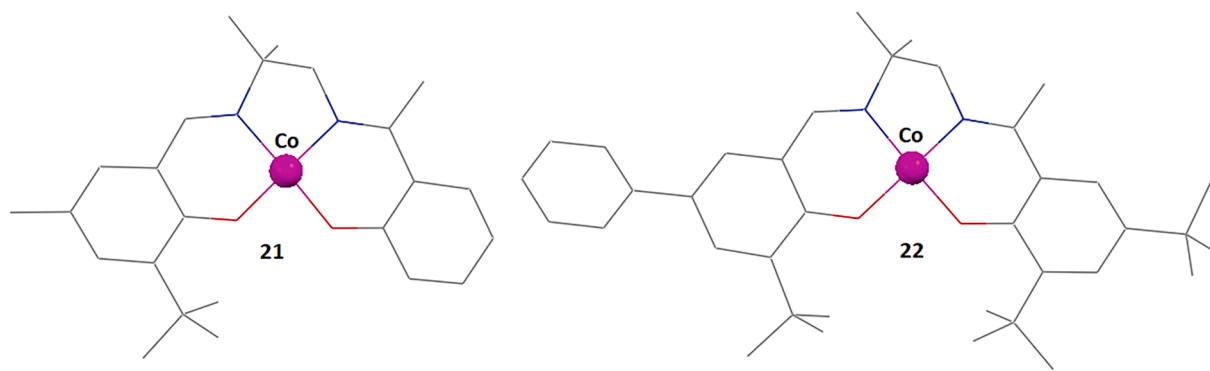


Fig. 7. Perspective views of **21** and **22**. Hydrogen atoms have been omitted for clarity.

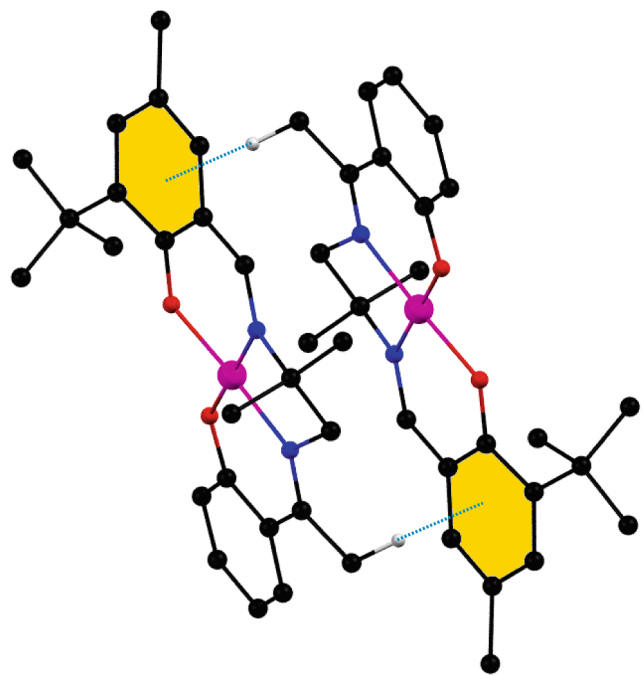


Fig. 8. The supra-molecular dimer of complex **21**, produced by the by C—H- $\pi$  interaction.

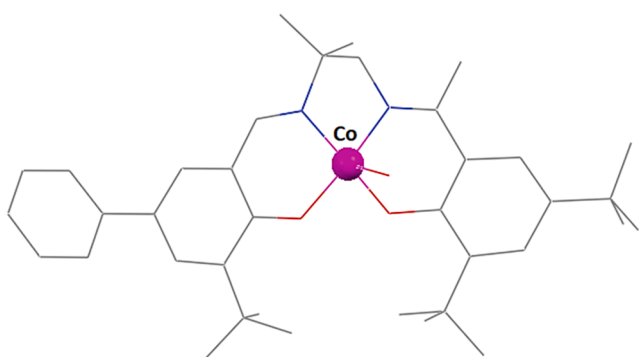


Fig. 9. The perspective view of the complex **23**. Hydrogen atoms, lattice water molecules and counter anion have been omitted for clarity.

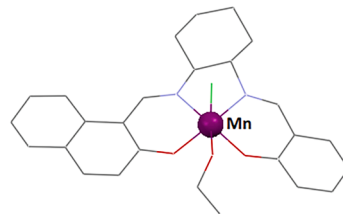


Fig. 10. Perspective view of complex **24**. Hydrogen atoms have been omitted for clarity.

## 6. Application of the complexes

One of the important applications of the complexes is to use the complexes as metallo-ligands to form poly-nuclear complexes. For example, complex **2** has been used to synthesis a series of carbonato bridged hetero-tetra-nuclear copper(III)-lanthanoid(III) complexes of general formula,  $[(\mu_4\text{-CO}_3)_2\{(\text{CuL})(\text{MeOH})\text{Ln}(\text{NO}_3)\}_2]$  ( $\text{Ln} = \text{Dy}, \text{Tb}$  and  $\text{Gd}$ ) on reaction with  $\text{Ln}(\text{NO}_3)_3\cdot 6\text{H}_2\text{O}$  salts in a slightly basic medium. The syntheses of these carbonato bridged complexes are also noteworthy as they are formed by spontaneous absorption of atmospheric  $\text{CO}_2$  ion. The magnetic properties of these tetra-nuclear complexes are also interesting. The dc magnetic susceptibility measurements indicate ferromagnetic interaction between copper(II) and lanthanoid(III) ions.  $\text{Cu}_2\text{Dy}_2$  and  $\text{Cu}_2\text{Tb}_2$  complexes show SMM behavior.  $\text{Cu}_2\text{Gd}_2$  complex shows an outstanding magneto-caloric effect [34]. The perspective view of  $[(\mu_4\text{-CO}_3)_2\{(\text{CuL}^{\prime})(\text{MeOH})\text{Dy}(\text{NO}_3)\}_2]$  has been shown in Fig. 12.

Complexes **14** and **15** have been used to prepare different nickel(II)-manganese(III) complexes of diverse nuclearities, e.g.  $[(\text{NiL}^{11})_2\text{Mn}(\text{N}_3)]\text{ClO}_4$ ,  $[(\text{NiL}^{11})_2\text{Mn}_2(\text{N}_3)_2(\mu_{1,1}\text{-N}_3)_2(\text{CH}_3\text{OH})_2]$ ,  $[(\text{NiL}^{11})_2\text{Mn}_2(\mu_{1,3}\text{-N}_3)(\text{H}_2\text{O})]\text{ClO}_4\cdot \text{CH}_3\text{OH}$ ,  $[(\text{NiL}^9)_2\text{Mn}(\text{N}_3)_2\cdot \text{CH}_3\text{CN}$ ,  $[(\text{NiL}^9)_2\text{Mn}(\text{N}_3)(\text{H}_2\text{O})]\text{ClO}_4\cdot \text{H}_2\text{O}$ ,  $[(\text{NiL}^9)_2\text{Mn}(\text{H}_2\text{O})_2(\mu_{1,3}\text{-N}_3)]\text{ClO}_4$  [40,41]. The perspective views of some of these complexes are shown in Fig. 13.

The packing of some complexes in the solid state has also been rationalized by theoretical molecular electrostatic potential surface (MEPS) calculations. For example, Significant roles of C—H— $\pi$  (chelate ring) and  $\pi$ - $\pi$ (chelate ring) interactions governing the crystal packing in complexes **3–6** have been estimate energetically by DFT calculations and have also been characterized using Bader's theory [35].

*In vitro* anti-proliferative effects of complex **9** {and 5-f-fluorouracil (5-FU) as a reference drug control} were determined against human liver cancer cell line (Hep-G2) by MTT assay. Results of MTT assay indicates considerable cytotoxic activity of complex **9** against Hep-G2 cells with  $\text{IC}_{50}$  (half maximum inhibitory concentration) value of  $7.0 \text{ } \mu\text{g mL}^{-1}$

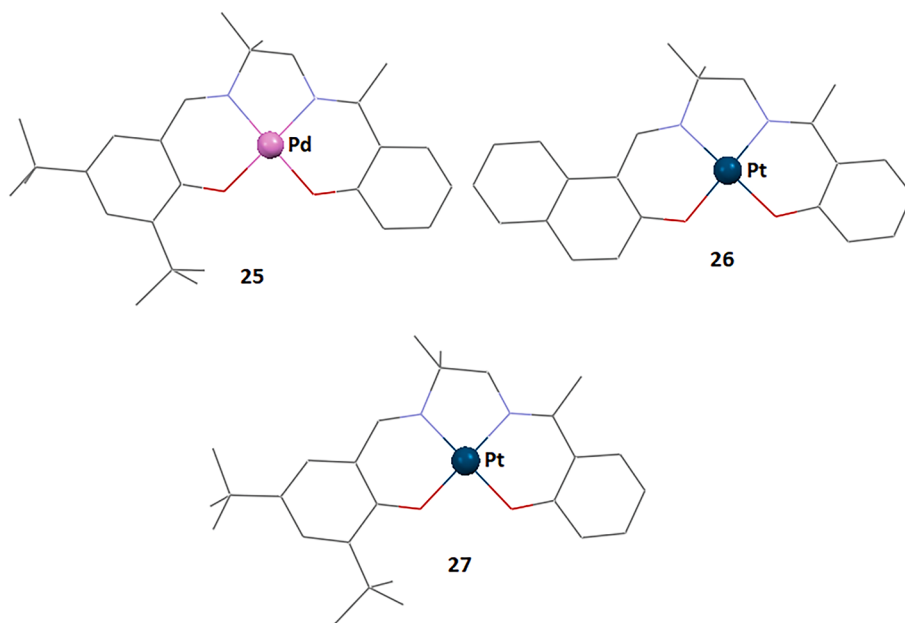


**Fig. 11.** The perspective view of the complexes [PdL<sup>15</sup>] (25), [PtL<sup>14</sup>]·CHCl<sub>3</sub>(26) and [PtL<sup>15</sup>] (27). Hydrogen atoms in all three complexes and lattice chloroform molecules in 26 have not been shown for clarity.

**Table 9**

The M–O<sub>phenoxo</sub> and M–N<sub>imine</sub> bond lengths (involving the salen type Schiff bases) around central metal centers in complexes 10–19. M = palladium(II) in complexes 25, M = platinum(II) in complexes 26 and 27.

Complexes	M–N <sub>imine</sub> (Å)	M–O <sub>imine</sub> (Å)	Ref
[PdL <sup>15</sup> ] (25)	1.955(2), 1.966(2)	1.997(2), 1.989(2)	43
[PtL <sup>14</sup> ]·CHCl <sub>3</sub> (26)	1.952(6), 1.954(6)	1.984(5), 1.993(5)	42
[PtL <sup>15</sup> ] (27)	1.961(4), 1.946(4)	1.993(3), 1.992(3)	43

**Table 10**

The  $\tau_4$  index of tetra-coordinated palladium(II) and platinum(II) complexes.

Complexes	Largest L–M–L angles (°)	2nd largest L–M–L angles (°)	$\tau_4$ index	Ref
25; M = Pd	177.82(8)	176.37(8)	0.04	43
26; M = Pt	179.6(2)	176.8(2)	0.03	42
27; M = Pt	179.11(15)	177.84(15)	0.02	43

[38].

Complexes 10–13 exhibit high affinities towards either a double stranded DNA (dsDNA) molecule D2, or the parallel unimolecular quadruplex DNA (qDNA) molecule Q1 [39].

The electronic spectra of complexes 16 and 26 showed characteristic absorption band around 500 nm, which may be assigned to the transition related to the  $\pi$ -conjugated system of the naphthalene moiety of the ligand. Complex 26 shows very good photo-luminescence. This may be related to the  $\pi$ -conjugated system of the naphthalene ring. Mechanochromic photo-luminescence has been observed for complex 17, 25 and 27 (i.e., micro-crystals of these complexes show photoemission of various colors in response to different mechanical stimuli) [43].

Complex 24 showed different bio-activities. The interaction of the complex with bovine serum albumin (BSA) can strongly quench the intrinsic fluorescence of BSA through a static quenching mechanism. Complex 24 also showed SOD (superoxide dismutase)-like activity and ABTS {2,2'-azinobis-(3-ethylbenzothiazoline-6-sulfonic acid)} free radical scavenging ability [49]. Superoxide scavenger activities of 24 and its BSA adduct were assayed by measuring (spectro-photometrically) the competition kinetics of nitro blue tetrazolium (NBT) (Scheme

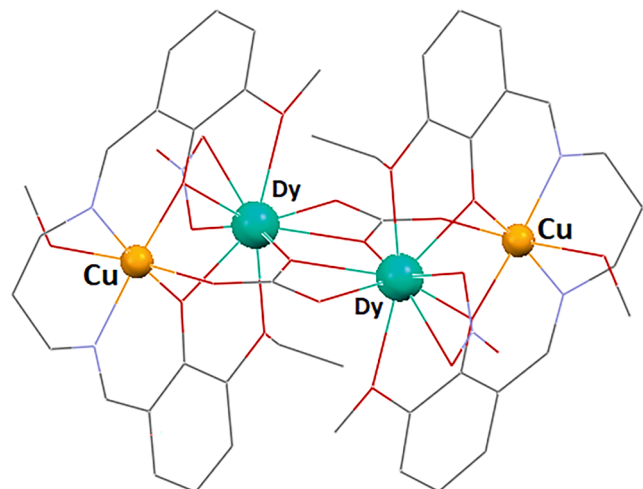


**Fig. 12.** The perspective view of the complex,  $[(\mu_4\text{-CO}_3)_2\{\text{CuL}^7\}(\text{MeOH})\text{Dy}(\text{NO}_3)_2]_2$ . Hydrogen atoms have been omitted for clarity. The cif has been retrieved from CCDC. CCDC number is 1935709.

40).

## 7. Future prospect

The most important aspect of the complexes, which is underutilized, is the use of the complexes as metallo-ligands for the synthesis of multi-metallic complexes. This is not at all explored in details. The multi-metallic complexes will be expected to be important as magnetic materials.

The theoretical study on the supramolecular architecture of the complexes in solid state is also not done thoroughly. For example, the pyridine rings in each of these complexes provide electron rich regions, which may be involved in cation–π interaction with the metal centers of neighbouring symmetry related molecules of the complexes. To explore other conventional and unconventional non-covalent interactions in the solid state structures of the complexes could also be an interesting task the theoretical chemists.

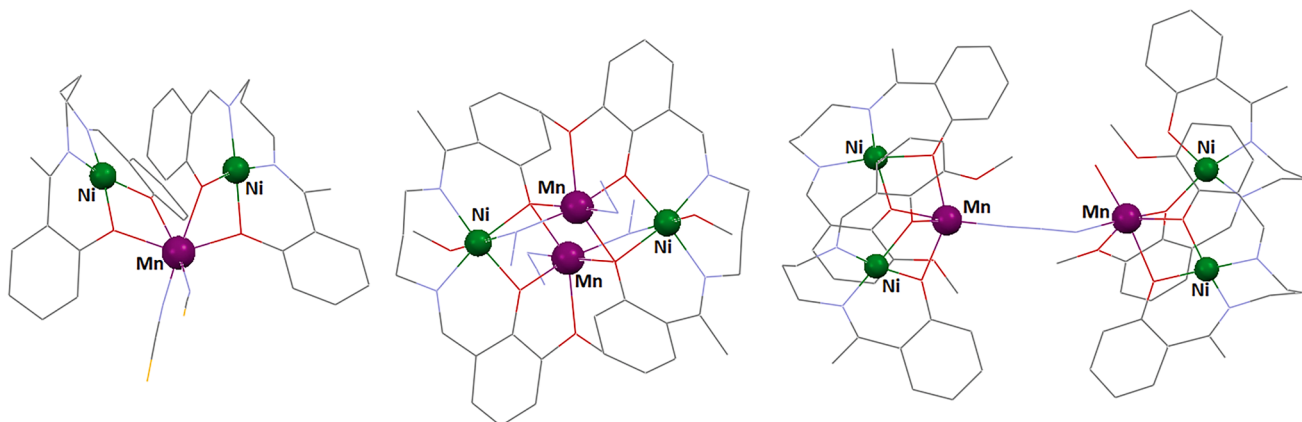
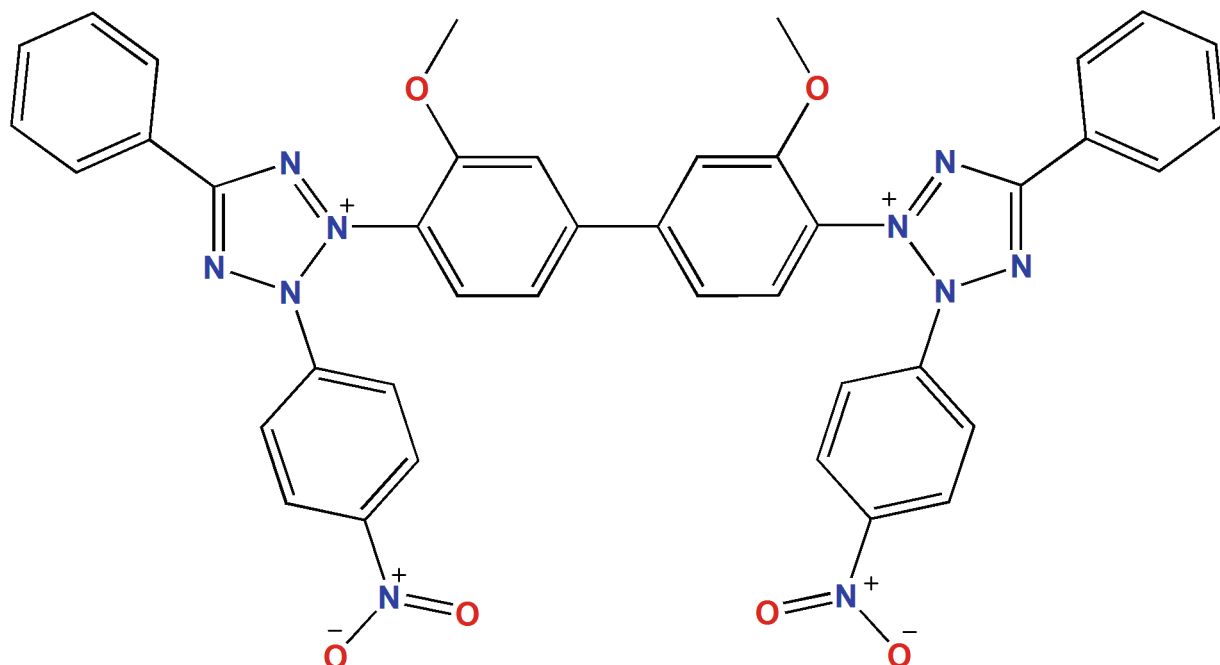


**Fig. 13.** Perspective view of tri-nuclear, tetra-nuclear and hexa-nuclear nickel(II)-manganese(III) complexes,  $[(\text{NiL}^9)_2\text{Mn}(\text{NCS})_2]\cdot\text{CH}_3\text{CN}$  (left),  $[(\text{NiL}^{11})_2\text{Mn}_2(\text{N}_3)_2(\mu 1,1-\text{N}_3)_2(\text{CH}_3\text{OH})_2]$  (middle),  $\{(\text{NiL}^{11})_2\text{Mn}_2(\mu 1,3-\text{N}_3)(\text{H}_2\text{O})\}\cdot(\text{CH}_3\text{OH}), (\text{ClO}_4)_3$  (right). Hydrogen atoms have been omitted for clarity. CCDC numbers are 1857026, 1,836,636 and 1,836,637 respectively.



**Scheme 40.** Schematic representation of nitro blue tetrazolium (NBT). The counter anions (usually chloride) are not shown.

The catalytic and enzyme-mimetic properties of the complexes were also not done for most of the complexes. This could be done by the material scientists and biological chemists in future to have some exciting data. The complexes are expected to be semiconducting in nature from the values of electronic absorption. Thus the conductance studies and application of the complexes in the fabrication of several opto-electronic devices could also be important.

This review will also help the synthetic inorganic chemists to have an idea on the fact that only a limited number of asymmetric Schiff bases have been used for the synthesis of transition metal complexes. So, a series of similar complexes could be synthesized easily following the same methodology just by changing the constituent diamines and aldehydes of the Schiff bases.

## 8. Summary and conclusion

Salen type salicylaldimine Schiff bases are very common to the synthetic inorganic chemists as very useful ligands for the synthesis of

various transition and non-transition metal complexes. The ligand system could easily be prepared by 1:2 condensation of a diamine and a suitable salicylaldehyde derivative. The ligand system may be considered as ‘symmetric’ in the sense that both the amine groups of the diamine in each of these ligand systems are condensed with the same salicylaldehyde moiety. On the other hand, synthesis of salen type ‘asymmetric’ Schiff bases (where two different salicylaldehyde derivatives are condensed with two amine groups of a diamine) is relatively less explored.

In this review, we have tried to highlight the synthetic strategy of salen type ‘asymmetric’ Schiff bases and their application in the synthesis of mono-nuclear transition metal complexes. Their important properties and applications of the complexes have also been discussed. The most important application of these mono-nuclear complexes is to use them as metallo-ligands for the synthesis of homo and hetero-poly-nuclear complexes exploiting the outstanding bridging ability of phenoxy oxygen atoms of the salicylaldimine ligands. These poly-nuclear complexes may be used as magnetic materials with diverse

applications. The review will help readers to have a gross knowledge regarding the recent development in synthetic and characterization of X-ray characterized transition metal complexes with ‘salen type’ asymmetric Schiff base ligands. The present review will also help the synthetic inorganic chemists and coordination chemists to work further in this particular field.

## Declaration of Competing Interest

The authors declare that they have no known competing financial interests or personal relationships that could have appeared to influence the work reported in this paper.

## Data availability

No data was used for the research described in the article.

## Acknowledgement

P.M. acknowledges UGC, India for providing Junior Research Fellowship.

## Appendix A. Supplementary data

Supplementary data to this article can be found online at <https://doi.org/10.1016/j.ica.2022.121246>.

## References

- [1] I. Mondal, S. Chattopadhyay, J. Coord. Chem. 72 (2019) 3183–3209.
- [2] S. Banerjee, P. Ghorai, P. Sarkar, A. Panja, A. Saha, Inorg. Chim. Acta 499 (2020), 119176.
- [3] P. Bhowmik, H.P. Nayek, M. Corbella, N. Aliaga-Alcalde, S. Chattopadhyay, Dalton Trans. 40 (2011) 7916–7926.
- [4] K. Ghosh, K. Harms, A. Bauzá, A. Frontera, S. Chattopadhyay, Dalton Trans. 47 (2018) 331–347.
- [5] P. Mukherjee, C. Biswas, M.G.B. Drew, A. Ghosh, Polyhedron 26 (2007) 3121–3128.
- [6] S. Ghosh, S. Biswas, A. Bauza, M. Barceló-Olivier, A. Frontera, A. Ghosh, Inorg. Chem. 52 (2013) 7508–7523.
- [7] P. Mahapatra, S. Ghosh, S. Giri, V. Rane, R. Kadam, M.G.B. Drew, A. Ghosh, Inorg. Chem. 56 (2017) 5105–5121.
- [8] A. Panja, N. Shaikh, P. Vojtíšek, S. Gao, P. Banerjee, N. J. Chem. 26 (2002) 1025–1028.
- [9] A. Panja, N. Shaikh, M. Ali, P. Vojtíšek, P. Banerjee, Polyhedron 22 (2003) 1191–1198.
- [10] R. Karmakar, C.R. Choudhury, G. Bravic, J.P. Sutter, S. Mitra, Polyhedron 23 (2004) 949–954.
- [11] S. Saha, A. Sasmal, C.R. Choudhury, C.J. Gómez-García, E. Garribba, S. Mitra, Polyhedron 69 (2014) 262–269.
- [12] T.K. Ghosh, P. Mahapatra, S. Jana, A. Ghosh, Cryst. Eng. Comm. 21 (2019) 4620–4631.
- [13] M. Karmakar, S. Chattopadhyay, J. Mol. Struct. 1186 (2019) 155–186.
- [14] N. Sarkar, M.G.B. Drew, K. Harms, A. Batuza, A. Frontera, S. Chattopadhyay, Cryst. Eng. Comm. 20 (2018) 1077–1086.
- [15] T. Basak, K. Ghosh, C.J. Gomez-García, S. Chattopadhyay, Polyhedron 146 (2018) 42–54.
- [16] S. Chattopadhyay, M.G.B. Drew, A. Ghosh, Eur. J. Inorg. Chem. (2008) 1693–1701.
- [17] K. Ghosh, S. Banerjee, S. Chattopadhyay, Cryst. Eng. Comm. 21 (2019) 6026–6037.
- [18] S. Chattopadhyay, G. Bocelli, A. Musatti, A. Ghosh, Inorg. Chem. Comm. 9 (2006) 1053–1057.
- [19] S. Roy, M.G.B. Drew, A. Bauza, A. Frontera, S. Chattopadhyay, N. J. Chem. 42 (2018) 6062–6076.
- [20] S. Biswas, R. Saha, A. Ghosh, Organometallics 31 (10) (2012) 3844–3850.
- [21] D. Majumdar, T.K. Pal, S.A. Sakib, S. Das, K. Bankura, D. Mishra, Inorg. Chem. Comm. 128 (2021), 108609.
- [22] M. Nayak, S. Sarkar, S. Hazra, H.A. Sparkes, J.A.K. Howard, S. Mohanta, Cryst. Eng. Comm. 13 (2011) 124–132.
- [23] S. Sarkar, S. Mohanta, RSC Adv. 1 (2011) 640–650.
- [24] S. Roy, A. Bhattacharyya, S. Purkait, A. Bouza, A. Frontera, S. Chattopadhyay, Dalton Trans. 45 (2016) 15048–15059.
- [25] T. Ghosh Dastidar, K. Ghosh, M.G.B. Drew, R.M. Gomila, A. Frontera, S. Chattopadhyay, Polyhedron 222 (2022), 115862.
- [26] A. Hazari, A. Ghosh, J. Ind. Chem. Soc. 95 (2018) 1597–1606.
- [27] K. Ghosh, K. Harms, S. Chattopadhyay, Polyhedron 123 (2017) 162–175.
- [28] S. Ghosh, A. Ghosh, Inorg. Chim. Acta 442 (2016) 64–69.
- [29] A. Hazari, L.K. Das, A. Bauza, A. Frontera, A. Ghosh, Dalton Trans. 45 (2016) 5730–5740.
- [30] M. Karmakar, S. Roy, S. Chattopadhyay, Polyhedron 215 (2022), 115652.
- [31] A. Banerjee, P. Ghosh, N. Chowdhury, S. Chattopadhyay, Polyhedron 218 (2022), 115756.
- [32] T.G. Dastidar, S. Chattopadhyay, Polyhedron 211 (2022), 115511.
- [33] D.S. Kurchavova, M.P. Karusheva, M.V. Novozhilovaa, I.V. Korniyakovb, V. A. Bykova, A.M. Timonova, Russ. J. Gen. Chem. 90 (2020) 921–923.
- [34] S. Maity, A. Mondal, S. Konar, A. Ghosh, Dalton Trans. 48 (2019) 15170–15183.
- [35] P. Mahapatra, A. Bauza, A. Frontera, M.G.B. Drew, A. Ghosh, Inorg. Chim. Acta 477 (2018) 89–101.
- [36] N.S. Gwaram, H. Khaledi, H. Mohd Ali, Acta Cryst. E66 (2010), m813.
- [37] M. Barwiolek, E. Szlyk, T.M. Muziola, T. Lisb, Dalton Trans. 40 (2011) 11012–11022.
- [38] M. Behzad, L.S. Ghomi, M. Damercheli, B. Mehravi, M.S. Ardestani, H.S. Jahromi, Z. Abbasi, J. C. Chem. 69 (2016) 2469–2481.
- [39] S.Q.T. Pham, C. Richardson, C. Kelso, A.C. Willis, S.F. Ralp, Dalton Trans. 49 (2020) 10360–10379.
- [40] M.G.B. Drew, A. Ghosh, Inorg. Chem. 57 (2018) 8338–8353.
- [41] P. Mahapatra, M.G.B. Drew, A. Ghosh, Dalton Trans. 47 (2018) 13957–13971.
- [42] H. Houjou, Y. Hoga, Y.L. Ma, H. Achira, I. Yoshikawa, T. Mutai, K. Matsumura, Inorg. Chim. Acta 461 (2017) 27–34.
- [43] H. Achira, Y. Hoga, I. Yoshikawa, T. Mutai, K. Matsumura, H. Houjou, Polyhedron 113 (2016) 123–131.
- [44] T.J. Dunn, L. Chiang, C.F. Ramogida, K. Hazin, M.I. Webb, M.J. Katz, T. Storr, Chem. Eur. J. 19 (2013) 9606–9618.
- [45] M. Barwiolek, E. Szlyk, A. Surdykowski, A. Wojtczak, Dalton Trans. 42 (2013) 11476–11487.
- [46] M.S. Seo, K. Kim, H. Kim, Chem. Commun. 49 (2013) 11623–11625.
- [47] A. Bottcher, H. Elias, B. Eisenmann, E. Hilms, A. Huber, R. Kniep, C. Rohr, Z. Naturforsch. B. Chem. Sci. 49b (1994) 1089–1100.
- [48] R.M. Clarke, K. Hazin, J.R. Thompson, D. Savard, K.E. Prosser, T. Storr, Inorg. Chem. 55 (2016) 762–774.
- [49] E. Zhang, Y. Wei, F. Huang, Q. Yu, H. Bian, H. Liang, F. Lei, J. Mole. Struc. 1155 (2018) 320–329.
- [50] L. Rigamonti, F. Demartin, A. Forni, S. Righetto, A. Pasini, Inorg. Chem. 45 (2006) 10976–10989.
- [51] A.W. Kleij, Dalton Trans. (2009) 4635–4639.
- [52] E.M. Opozdaa, W. Łasochab, B.W. Gajda, Anorg. Allg. Chem. 630 (2004) 597–603.
- [53] R. Atkins, G. Brewer, E. Kokot, G.M. Mockler, E. Sinn, Inorg. Chem. 24 (1985) 127–134.
- [54] P. Mahapatra, S. Ghosh, N. Koizumi, T. Kanetomo, T. Ishida, M.G.B. Drew, A. Ghosh, Dalton Trans. 46 (2017) 12095–12105.
- [55] S. Chattopadhyay, M.S. Ray, S. Chaudhuri, G. Mukhopadhyay, G. Bocelli, A. Cantoni, A. Ghosh, Inorg. Chim. Acta. 359 (2006) 1367–1375.
- [56] A.W. Addison, T.N. Rao, J. Reedijk, J. van Rijn, G.C. Verschoor, J. Chem. Soc. Dalton Trans. (1984) 1349–1356.
- [57] S. Chattopadhyay, G. Bocelli, A. Cantoni, A. Ghosh, Inorg. Chim. Acta 359 (2006) 4441–4446.
- [58] L. Yang, D.R. Powell, R.P. Houser, Dalton Trans. (2007) 955–964.